Physics Informed Neural Networks for solving Dirac equation in (1+1) dimension

by

Aigerim Bazarkhanova

Submitted to the Department of Mathematics
in partial fulfillment of the requirements for the degree of

Master of Science in Applied Mathematics

at the

NAZARBAYEV UNIVERSITY

May 2021

Author . . . .
Department of Mathematics

Certified by . . . .
Alejandro Castilla
Assistant Professor
Thesis Supervisor

Accepted by . . . .
Daniel Pugh
Dean, School of Sciences and Humanities

PHYSICS INFORMED NEURAL NETWORKS FOR SOLVING DIRAC EQUATION IN (1+1) DIMENSION

AIGERIM BAZARKHANOVA

Abstract. The Dirac equation plays a fundamental role in quantum physics and its exact solutions are of utmost importance. In this study we solved Linear and Nonlinear Dirac equation in (1+1) dimension and obtained analytical solutions. Moreover we have implemented Physics Informed Neural Networks to get approximate solutions of Linear and Nonlinear Dirac equation in (1+1) dimension. During the experiments we observed that Physics Informed Neural Networks are not capable of providing good solutions for any given time and faced the problem of choosing appropriate weights for each loss function. Therefore, architecture of multilayer feedforward neural networks for approximating solutions of Dirac equation needs further investigation.

Contents

Last modification: Wednesday 5$^{\text{th}}$ May, 2021.

Acknowledgments

In this section I would like to mention important people who contributed to this research during preparatory stages. I would like to express my sincere gratitude to my supervisor Dr. Alejandro Castilla, who guided me through the whole research process, for his kind responsiveness and patience. I would like to give special thanks to my Second Reader Dr. Zhenisbek Assylbekov for helping me with applying Neural Networks to Dirac equation, choosing an appropriate literature and for agreeing to be a thesis committee member and to review the Thesis.

1. Introduction

Fast development of machine learning techniques is affecting both scientific and industry spheres and showing its high performance in making predictions for a given problem. These achievements have been tested in image, speech and voice recognition and are actively applied in other fields too. Since the main idea of the neural networks is to mimic human brain and train them to make accurate predictions, gradually most scientific and engineering fields are trying to get involved in machine learning.

In our study we consider exact and predicted solutions of Linear and Nonlinear Dirac equation in (1+1) dimension and also we estimate their error. The Dirac equation plays a fundamental role in quantum mechanics and describes spin 1/2 particles, in addition to neutrons, electrons and protons.

Relativistic quantum mechanical descriptions of an electron were of great interest for scholars and they have conducted enormous research to find out an equation which can describe its behaviour. One of the first attempts was to express the energy as a function of particle momentum mass:

$$E = \sqrt{(pc)^2 + (mc^2)^2}, \tag{1}$$

which has been used as a basis of relativistic quantum mechanics. Next step was developing relativistic wave equation and they have used expression of relativistic energy relation (1) by substituting energy and momentum operators and applying operators to both sides of wave function, which lead to

$$i\hbar\partial_t\psi = [\sqrt{(-\hbar c)^2\nabla^2 + (mc^2)^2}]\psi.$$

This is the Klein - Gordon equation and they have encountered with a problem that it provided solutions with negative energy and also the square root was hard to interpret in quantum mechanics. Nevertheless this issue has been solved by British physicist and Nobel Prize winner Paul Dirac in 1928. He converted the second order linear partial differential equation into a system of first order partial differential equations avoiding the square root

$$i\hbar\partial_t\psi = \left(-i\hbar c\hat{\alpha}\cdot\nabla + \beta mc^2\right)\psi, \tag{2}$$

or, equivalently

$$\frac{1}{c}\gamma^{(0)}\partial_t\psi + (\gamma^{(j)}\cdot\nabla)\psi + i\kappa\psi = 0, \tag{3}$$

where $\kappa = \frac{mc}{\hbar}$, c is the speed of light, m is the mass of an electron, $\hbar$ is a Plank constant and explicit forms of Dirac matrices are as follows

$$\gamma^{(0)} = \beta, \quad \gamma^{(1)} = \beta\alpha_1, \quad \gamma^{(2)} = \beta\alpha_2, \quad \gamma^{(3)} = \beta\alpha_3,$$

where

$$\alpha_1 = \begin{bmatrix} 0 & 0 & 0 & 1 \\ 0 & 0 & 1 & 0 \\ 0 & 1 & 0 & 0 \\ 1 & 0 & 0 & 0 \end{bmatrix}, \qquad \alpha_2 = \begin{bmatrix} 0 & 0 & 0 & -i \\ 0 & 0 & i & 0 \\ 0 & -i & 0 & 0 \\ i & 0 & 0 & 0 \end{bmatrix}$$

$$\alpha_3 = \begin{bmatrix} 0 & 0 & 1 & 0 \\ 0 & 0 & 0 & -1 \\ 1 & 0 & 0 & 0 \\ 0 & -1 & 0 & 0 \end{bmatrix}, \qquad \beta = \begin{bmatrix} 1 & 0 & 0 & 0 \\ 0 & 1 & 0 & 0 \\ 0 & 0 & -1 & 0 \\ 0 & 0 & 0 & -1 \end{bmatrix}.$$

As a result we obtain the system of first order partial differential equations, where $\psi = \psi(x, y, z; t)$

$$\begin{cases} \frac{1}{c}\partial_t\psi_1 + \partial_x\psi_4 - i\partial_y\psi_4 + \partial_z\psi_3 + i\kappa\psi_1 = 0, \\ \frac{1}{c}\partial_t\psi_2 + \partial_x\psi_3 + i\partial_y\psi_3 - \partial_z\psi_4 + i\kappa\psi_2 = 0, \\ \frac{1}{c}\partial_t\psi_3 - \partial_x\psi_2 + i\partial_y\psi_2 - \partial_z\psi_2 + i\kappa\psi_3 = 0, \\ \frac{1}{c}\partial_t\psi_4 - \partial_x\psi_1 - i\partial_y\psi_1 + \partial_z\psi_1 + i\kappa\psi_4 = 0. \end{cases}$$

Hence, finding solutions of the Dirac equation requires finding solutions of the of system of partial differential equations [4], and multiple studies have been conducted to obtain exact and numerical solutions of the Dirac equation.

In 1990, physicists V.G. Bagrov and D. Gitman [2] published their book where they showed physical significance of relativistic wave equations and their exact solutions. Lately, in 2000 W. Greiner [7] presented his studies on the solutions of equations of relativistic quantum mechanics. Moreover, [13] has studied initial boundary value problem for the cubic Nonlinear Dirac equation in one space dimension with Dirichlet boundary conditions. Furthermore [15] has provided new exact analytic stationary solutions of the massive nonlinear Dirac equation in (1+1) dimensions as described by Thirring and Gross Neveu models. Also, [19] have studied an initial boundary value problem for a class of nonlinear Dirac equations with cubic terms, which include the equations for the massive Thirring model and the massive Gross-Neveu model.

In our study to simplify the problem we have decided to study Dirac equation in (1+1) dimension which may be written as

$$i\hbar\partial_t\Psi(x,t) = (-i\hbar c\alpha\partial_x + mc^2\beta)\Psi(x,t), \tag{4}$$

where Ψ denotes a two-component spinor depending upon $x \in R$ and upon time t. α and β are hermitian (2×2) matrices satisfying $\beta^2 = \alpha^2 = \mathbb{I}$ and anticommutation relation $\alpha\beta + \beta\alpha = 0$. A particular representation of the matrices α and β is given by [13]:

$$\alpha = \begin{bmatrix} 0 & 1 \\ 1 & 0 \end{bmatrix}, \quad \beta = \begin{bmatrix} 1 & 0 \\ 0 & -1 \end{bmatrix}.$$

Dirac equation in (1+1) dimension can be written as the system of equations:

$$\begin{cases} \frac{1}{c}\partial_t\psi_1(x,t) + \partial_x\psi_2(x,t) + i\kappa\psi_1(x,t) = 0, \\ -\frac{1}{c}\partial_t\psi_2(x,t) - \partial_x\psi_1(x,t) + i\kappa\psi_2(x,t) = 0. \end{cases} \tag{5}$$

For convenience purposes we can avoid physical constants by applying the following change of variables:

$$t = c\kappa\tau, \qquad x = \kappa\xi,$$

which leads to:

$$\begin{cases} \partial_\tau\psi_1(\xi,\tau) + \partial_\xi\psi_2(\xi,\tau) + i\psi_1(\xi,\tau) = 0, \\ -\partial_\tau\psi_2(\xi,\tau) - \partial_\xi\psi_1(\xi,\tau) + i\psi_2(\xi,\tau) = 0. \end{cases} \tag{6}$$

Solving partial differential equations analytically is not always possible and numerical methods are of utmost importance. Moreover, these days application of neural networks is being popular among scholars and extensive research has been done in applying them for solving partial differential equations. In 1989, [8] provided the mathematical proof that multilayer feedforward neural networks are capable of solving differential equations and named them as *universal function approximators*.

Researchers have actively started testing the model to several differential equations and comparing it with exact solutions with different numbers of hidden units. For instance, in 1994 [5] tested it for a linear Poisson equation and [1] for a heat equation. After 4 years in 1998 [10] they described artificial neural networks for solving ordinary and partial differential equations. Furthermore in 2001 [1] also mentioned an approximation power of neural networks in solving differential equations. In 2009 [16] provided a scheme of neural network architecture for solving Nonlinear Schrödinger equation and pointed out that quantum mechanics equations are obtaining great popularity among researchers and one of them is the research conducted by [12]. Also, in 2018 [17] offered deep learning algorithm for solving partial differential equations and provide examples of Hamilton-Jacobi-Bellman and Burgers equations. Studies have been conducted for Laplace, Poisson, Navier - Stokes and Nonlinear Schrödinger equation in [11] and Klein - Gordon equation in [9].

In this thesis we mostly follow the idea of [14]. They have named their neural networks as *Physics Informed Neural Networks (PINNs)* and obtained results which predicted solutions of Burgers equation, Nonlinear Schrödinger equation, Allen - Cahn equation and Navier - Stokes equation coincide with the exact solutions.

It can be seen that extensive research has been done to show the approximation power of the artificial neural networks and scholars are trying to find the most efficient method which will take less time and show high accuracy.

Outline of the thesis is as follows. In Section 2 we will consider Linear Dirac equation in (1+1) dimension, its plane wave solutions and solutions of initial value and initial boundary value problems. Next Section is devoted to solving Nonlinear Dirac equation in (1+1) dimension and Section 4 will demonstrate machine learning technique for solving Dirac equation in (1+1) dimension and process of creating the model.

2. Linear Dirac equation in (1+1) dimension

This section is devoted to solving Dirac equation in (1+1) dimension:

$$\begin{cases} \partial_\tau\psi_1(\xi,\tau)+\partial_\xi\psi_2(\xi,\tau)+i\psi_1(\xi,\tau)=0,\\ -\partial_\tau\psi_2(\xi,\tau)-\partial_\xi\psi_1(\xi,\tau)+i\psi_2(\xi,\tau)=0. \end{cases}$$

Here we consider plane wave solutions in Section 2.1, initial value problem in a line in Section 2.2 and finally provide solution for the initial boundary value problem in Section 2.3.

2.1. **Plane wave solutions.**

Lemma 2.1. *The Dirac equation in (1+1) dimension*

$$\begin{cases} \partial_\tau\psi_1(\xi,\tau)+\partial_\xi\psi_2(\xi,\tau)+i\psi_1(\xi,\tau)=0,\\ -\partial_\tau\psi_2(\xi,\tau)-\partial_\xi\psi_1(\xi,\tau)+i\psi_2(\xi,\tau)=0, \end{cases} \tag{7}$$

admits, for any $\xi\in\mathbb{R}$ and $\tau\in\mathbb{R}$, plane wave solutions of the form:

$$\psi_j(\xi,\tau)=a_j\exp\left[i(k\xi-\omega\tau)\right],\quad j=1,2, \tag{8}$$

provided that

i) $k^2=\omega^2-1,\quad a_1=\frac{a_2(1+\omega)}{k},\quad$ *for* $a_2\in\mathbb{R}$ *and* $\omega\neq\pm1$*; or*

ii) $k=-\frac{2a_1a_2}{a_2^2-a_1^2},\quad \omega=-\frac{2(a_1^2+a_2^2)}{a_2^2-a_1^2},\quad$ *for* $a_1,a_2\in\mathbb{R}$ *satisfying* $a_2^2-a_1^2\neq0$.

Proof. We can divide our proof into several steps:

Step 1. Finding necessary components of our equation:

First component of equation is its partial derivatives with respect to τ and ξ:

$$\partial_\tau\psi(\xi,\tau)=\begin{cases}-i\omega a_1e^{i(k\xi-\omega\tau)},\\ -i\omega a_2e^{i(k\xi-\omega\tau)}\end{cases},\partial_\xi\psi(\xi,\tau)=\begin{cases}ika_1e^{i(k\xi-\omega\tau)},\\ ika_2e^{i(k\xi-\omega\tau)}.\end{cases}$$

Step 2. Substitution of components to equation (6)

$$\begin{bmatrix}-i\omega a_1e^{i(k\xi-\omega\tau)}\\ i\omega a_2e^{i(k\xi-\omega\tau)}\end{bmatrix}+\begin{bmatrix}ika_2e^{i(k\xi-\omega\tau)}\\ -ika_1e^{i(k\xi-\omega\tau)}\end{bmatrix}+\begin{bmatrix}ia_1e^{i(k\xi-\omega\tau)}\\ ia_2e^{i(k\xi-\omega\tau)}\end{bmatrix}=\begin{bmatrix}0\\0\end{bmatrix}.$$

Divide $ie^{i(k\xi-\omega\tau)}$:

$$\begin{bmatrix}-\omega a_1\\ \omega a_2\end{bmatrix}+\begin{bmatrix}ka_2\\ -ka_1\end{bmatrix}+\begin{bmatrix}a_1\\ a_2\end{bmatrix}=0.$$

In our system of equations we have 4 unknowns which are ω,k,a_1 and a_2.

$$\begin{cases}-\omega a_1+ka_2+a_1=0,\\ \omega a_2-ka_1+a_2=0\end{cases} \tag{9}$$

Let's solve (9) in k and ω. Hence we can factor out a_1 and a_2 :

$$\begin{cases}a_1(1-\omega)+ka_2=0,\\ -ka_1+a_2(1+\omega)=0\end{cases}$$

Here we can check the determinant which must be zero to obtain solutions:

$$\begin{vmatrix}1-\omega & k\\ -k & 1+\omega\end{vmatrix}=1-\omega^2+k^2=0$$

From the second part of the system we can express a_1 as follows:

$$a_1 = \frac{a_2(1+\omega)}{k}$$

and plug in to the first part:

$$\frac{a_2(1+\omega)(1-\omega)}{k} + ka_2 = 0$$

which leads to :

$$a_2\left(1-\omega^2+k^2\right) = 0.$$

Here we assume that $a_2 \neq 0$ as we have to fix a_2 and $k^2 = \omega^2 - 1$.

Now let's check the second case and multiply first part of the system (9) to a_2 and second part to a_1 :

$$\begin{cases} -\omega a_1 a_2 + ka_2^2 + a_1 a_2 = 0, \\ \omega a_2 a_1 - ka_1^2 + a_2 a_1 = 0. \end{cases}$$

We can first sum them up and subtract:

$$\begin{cases} ka_2^2 - ka_1^2 + 2a_1 a_2 = 0, \\ -2\omega a_1 a_2 + ka_1^2 + ka_2^2 = 0. \end{cases}$$

From the fist part of the above system we obtain:

$$k = -\frac{2a_1 a_2}{a_2^2 - a_1^2}$$

Plugging in found k to the second part leads to:

$$\omega = -\frac{2\left(a_1^2 + a_2^2\right)}{a_2^2 - a_1^2}$$

□

2.2. **Initial Value Problem.** The purpose of this subsection is to provide solution of initial value problem for Linear Dirac equation in (1+1) dimension for any $\xi \in \mathbb{R}$ and $\tau > 0$.

Proposition 2.2. *The solution of the initial value problem of the linear Dirac equation in (1+1) dimension for any $\xi \in \mathbb{R}$ and $\tau > 0$*

$$\begin{cases} \partial_\tau \psi_1(\xi,\tau) + \partial_\xi \psi_2(\xi,\tau) + i\psi_1(\xi,\tau) = 0, \\ -\partial_\tau \psi_2(\xi,\tau) - \partial_\xi \psi_1(\xi,\tau) + i\psi_2(\xi,\tau) = 0, \end{cases} \tag{10}$$

with initial conditions

$$\psi_1(\xi,0) = f(\xi) \quad \textit{and} \quad \psi_2(\xi,0) = g(\xi)$$

is given by

$$\psi_1(\xi,\tau) = \frac{2i}{2\pi}\int_{\mathbb{R}}\Big[\int_{\mathbb{R}} e^{i\theta(\xi-y)}\frac{-\theta}{2\sqrt{1+\theta^2}}\sin\left(\tau\sqrt{1+\theta^2}\right)d\theta\Big]g(y)\,dy$$
$$+\frac{1}{2\pi}\int_{\mathbb{R}}\int_{\mathbb{R}} e^{i\theta(\xi-y)}\frac{1}{2\sqrt{1+\theta^2}}\Big[(1+\sqrt{1+\theta^2})e^{-i\sqrt{1+\theta^2}\tau} - (1-\sqrt{1+\theta^2})e^{i\sqrt{1+\theta^2}\tau}d\theta\Big]f(y)dy$$

and

$$\psi_2(\xi,\tau) = \frac{2i}{2\pi}\int_{\mathbb{R}}\Big[\int_{\mathbb{R}} e^{i\theta(\xi-y)}\frac{-\theta}{2\sqrt{1+\theta^2}}\sin\left(\tau\sqrt{1+\theta^2}\right)d\theta\Big]f(y)\,dy$$
$$+\frac{1}{2\pi}\int_{\mathbb{R}}\int_{\mathbb{R}} e^{i\theta(\xi-y)}\frac{1}{2\sqrt{1+\theta^2}}\Big[(1+\sqrt{1+\theta^2})e^{i\sqrt{1+\theta^2}\tau} - (1-\sqrt{1+\theta^2})e^{-i\sqrt{1+\theta^2}\tau}d\theta\Big]g(y)dy$$

Proof. Let's divide our proof to the following steps:

Step 1:

Remember that if f is integrable function on $\mathbb{R}$, its Fourier Transform is the function $\hat{f}$ defined by

$$\hat{f}(\theta) = \int e^{-i\theta\xi} f(\xi) d\xi.$$

Furthermore if f is continuous and piecewise smooth $f' \in L^2$, then

$$[\hat{f'}](\theta) = i\theta \hat{f}(\theta). \tag{11}$$

Hence, according to (11) the Fourier transform converts differentiation into a simple algebraic operation and by using this fact we can reduce the system of partial differential equations to easily solvable system of ordinary differential equations.

$$[\hat{f}'_\xi](\theta) = \int e^{-i\theta\xi} f'(\xi) d\xi = -\int (i\theta) e^{-i\theta\xi} f(\xi) d\xi = i\theta f(\hat{\theta}).$$

Step 2: Applying Fourier transform:

$$\partial_\tau \hat{\psi}(\theta,\tau) = \begin{bmatrix} \partial_\tau \hat{\psi}_1(\theta,\tau) \\ \partial_\tau \hat{\psi}_2(\theta,\tau) \end{bmatrix}, \quad \partial_\xi \hat{\psi}(\theta,\tau) = \begin{bmatrix} i\theta \hat{\psi}_1(\theta,\tau) \\ i\theta \hat{\psi}_2(\theta,\tau) \end{bmatrix}$$

Since we obtained necessary components of our plane wave equation, we can substitute them to (12)

$$\begin{bmatrix} \partial_\tau \hat{\psi}_1(\theta,\tau) \\ -\partial_\tau \hat{\psi}_2(\theta,\tau) \end{bmatrix} + \begin{bmatrix} i\theta \hat{\psi}_2(\theta,\tau) \\ -i\theta \hat{\psi}_1(\theta,\tau) \end{bmatrix} + \begin{bmatrix} i\hat{\psi}_1(\theta,\tau) \\ i\hat{\psi}_2(\theta,\tau) \end{bmatrix} = \begin{bmatrix} 0 \\ 0 \end{bmatrix}.$$

Step 3: For convenience purposes let's make following replacement:

$$\begin{bmatrix} \partial_\tau \psi_1(\xi,\tau), \\ \partial_\tau \psi_2(\xi,\tau) \end{bmatrix} = \begin{bmatrix} u_1'(\tau) \\ u_2'(\tau) \end{bmatrix},$$

$$\begin{bmatrix} u_1'(\tau) \\ -u_2'(\tau) \end{bmatrix} + \begin{bmatrix} i\theta u_2(\tau) \\ -i\theta u_1(\tau) \end{bmatrix} + \begin{bmatrix} iu_1(\tau) \\ iu_2(\tau) \end{bmatrix} = \begin{bmatrix} 0 \\ 0 \end{bmatrix}$$

$$\begin{bmatrix} u_1'(\tau) \\ u_2'(\tau) \end{bmatrix} = \begin{bmatrix} -i & -i\theta \\ -i\theta & i \end{bmatrix} \begin{bmatrix} u_1(\tau) \\ u_2(\tau) \end{bmatrix} \tag{12}$$

To find solutions explicitly we assume that $u = \eta e^{rt}$ and substitute for u in (12). We are led to the system of algebraic equations ([3], Ch. 7, p.385)

$$\begin{bmatrix} -i-r & -i\theta \\ -i\theta & i-r \end{bmatrix} \begin{bmatrix} \eta_1 \\ \eta_2 \end{bmatrix} = \begin{bmatrix} 0 \\ 0 \end{bmatrix}. \tag{13}$$

Equations have a nontrivial solution if and only if the determinant is zero. Thus, acceptable values of r are found from the equation:

$$\begin{vmatrix} -i-r & -i\theta \\ -i\theta & i-r \end{vmatrix} = (-i-r)(i-r) - (i\theta)^2 = 1 + r^2 + \theta^2.$$

Equations have the roots: $r_{1,2} = \pm i\sqrt{\theta^2+1}$ and these are the eigenvalues of the matrix in equation (13). Now we have to find corresponding eigenvalues:

Case r_1 :

$$\begin{bmatrix} -i - i\sqrt{\theta^2+1} & -i\theta \\ -i\theta & i - i\sqrt{\theta^2+1} \end{bmatrix} \begin{bmatrix} \eta_1 \\ \eta_2 \end{bmatrix} = \begin{bmatrix} 0 \\ 0 \end{bmatrix}.$$

There is an infinite family of eigenvectors , corresponding to the eigenvalue r_1. We will choose a single member of this family as a representative in the rest ([3], Ch. 7, p.385) and obtain that:

$$\eta_1 = 1, \eta_2 = -\frac{1+\sqrt{\theta^2+1}}{\theta}$$

Case r_2:

$$\begin{bmatrix} -i + i\sqrt{\theta^2+1} & -i\theta \\ -i\theta & i + i\sqrt{\theta^2+1} \end{bmatrix} \begin{bmatrix} \eta_1 \\ \eta_2 \end{bmatrix} = \begin{bmatrix} 0 \\ 0 \end{bmatrix}.$$

Here also each row of this vector leads to the condition $\eta_1 - \eta_2 = 0$, so η_1 and η_2 are equal but their value is not determined. Thus, we reveal that we can choose η_1 as 1. Thus,

$$\eta_1 = 1, \eta_2 = \frac{\sqrt{\theta^2+1}-1}{\theta}.$$

As a result we obtain following solution in $u(\tau)$

$$u(\tau) = C_1 \begin{pmatrix} 1 \\ \frac{-1-\sqrt{\theta^2+1}}{\theta} \end{pmatrix} e^{i\sqrt{1+\theta^2}\tau} + C_2 \begin{pmatrix} 1 \\ \frac{-1+\sqrt{\theta^2+1}}{\theta} \end{pmatrix} e^{-i\sqrt{1+\theta^2}\tau}.$$

Step 4 Our next step is applying initial conditions

$$\begin{cases} \hat{\psi}_1(\theta,0) = \hat{f}(\theta), \\ \hat{\psi}_2(\theta,0) = \hat{g}(\theta) \end{cases}$$

which leads to

$$\begin{cases} C_1 + C_2 = \hat{f}(\theta), \\ \frac{-1-\sqrt{1+\theta^2}}{\theta} C_1 - \frac{1-\sqrt{1+\theta^2}}{\theta} C_2 = \hat{g}(\theta) \end{cases} \tag{14}$$

Our aim is to find out C_1 and C_2, and we can express C_1 in terms of C_2 and $\hat{f}(\theta)$:

$$C_1 = \hat{f}(\theta) - C_2,$$

and plug in to the second part of our system (14)

$$\frac{-1-\sqrt{1+\theta^2}}{\theta}(\hat{f}(\theta) - C_2) - \frac{1-\sqrt{1+\theta^2}}{\theta} C_2 = \hat{g}(\theta).$$

From the above equation we can express C_2 in terms of $g(\hat{\theta})$ and $f(\hat{\theta})$ which is following:

$$C_2 = \frac{\hat{g}(\theta)\theta + (1+\sqrt{1+\theta^2})\hat{f}(\theta)}{2\sqrt{1+\theta^2}}. \tag{15}$$

Our next step is finding C_1 by plugging in (15) to $C_1 = f(\hat{\theta}) - C_2$ which leads to :

$$C_1 = \hat{f}(\theta) - C_2 = \hat{f}(\theta) - \frac{\hat{g}(\theta)\theta + (1+\sqrt{1+\theta^2})\hat{f}(\theta)}{2\sqrt{1+\theta^2}}.$$

After making some arithmetic simplifications, we obtain that

$$C_1 = -\frac{\hat{g}(\theta)\theta + \hat{f}(\theta)(1-\sqrt{1+\theta^2})}{2\sqrt{1+\theta^2}}.$$

As a result, we see that our constants C_1 and C_2 are as follows:

$$C_1 = -\frac{\hat{g}(\theta)\theta + \hat{f}(\theta)(1-\sqrt{1+\theta^2})}{2\sqrt{1+\theta^2}}, \quad C_2 = \frac{\hat{g}(\theta)\theta + (1+\sqrt{1+\theta^2})\hat{f}(\theta)}{2\sqrt{1+\theta^2}}.$$

Step 5 Now we use Fourier inversion theorem to find a solution ([6], Ch.7, p.218)

(16) $$f(x) = \frac{1}{2\pi}\int e^{i\theta x}\hat{f}(\theta)d\theta.$$

Referring to (16) we have that:

$$\psi(\xi,\tau) = \frac{1}{2\pi}\int\limits_R e^{i\theta\xi}\hat{\psi}(\theta,\tau)d\theta = \frac{1}{2\pi}\int\limits_R e^{i\theta\xi}\begin{bmatrix}\hat{\psi}_1(\theta,\tau)\\ \hat{\psi}_2(\theta,\tau)\end{bmatrix}d\theta,$$

here we may use results from (16) to find $\psi(x,t)$.

$$\psi_1(\xi,\tau) = \frac{1}{2\pi}\int_{\mathbb{R}} e^{i\theta\xi}\hat{\psi}_1(\theta,\tau)d\theta =$$

$$\frac{1}{2\pi}\int_{\mathbb{R}} e^{i\theta\xi}\Big(-\frac{\theta\hat{g}(\theta)+\hat{f}(\theta)(1-\sqrt{1+\theta^2})}{2\sqrt{1+\theta^2}}e^{i\sqrt{1+\theta^2}\tau}+\frac{\hat{g}(\theta)\theta+(1+\sqrt{1+\theta^2})\hat{f}(\theta)}{2\sqrt{1+\theta^2}}e^{-i\sqrt{1+\theta^2}\tau}\Big)\,d\theta =$$

$$\frac{1}{2\pi}\int_{\mathbb{R}} e^{i\theta\xi}\frac{-\theta}{2\sqrt{1+\theta^2}}\Big(e^{i\sqrt{1+\theta^2}\tau}-e^{-i\sqrt{1+\theta^2}\tau}\Big)\widehat{g}(\theta)\,d\theta +$$

$$+\frac{1}{2\pi}\int_{\mathbb{R}}\frac{e^{i\theta\xi}}{2\sqrt{1+\theta^2}}\Big((1+\sqrt{1+\theta^2})e^{-i\sqrt{1+\theta^2}\tau}-(1-\sqrt{1+\theta^2})e^{i\sqrt{1+\theta^2}\tau}\Big)\widehat{f}(\theta)\,d\theta =$$

$$\frac{1}{2\pi}\int_{\mathbb{R}} e^{i\theta\xi}\frac{-\theta}{2\sqrt{1+\theta^2}}\Big(e^{i\sqrt{1+\theta^2}\tau}-e^{-i\sqrt{1+\theta^2}\tau}\Big)\int_{\mathbb{R}} e^{-i\theta y}g(y)\,dy\,d\theta$$

$$+\frac{1}{2\pi}\int_{\mathbb{R}}\frac{e^{i\theta\xi}}{2\sqrt{1+\theta^2}}\Big((1+\sqrt{1+\theta^2})e^{-i\sqrt{1+\theta^2}\tau}-(1-\sqrt{1+\theta^2})e^{i\sqrt{1+\theta^2}\tau}\Big)\int_{\mathbb{R}} e^{-i\theta y}f(y)dy\,d\theta$$

$$= \frac{1}{2\pi}\int_{\mathbb{R}}\int_{\mathbb{R}} e^{i\theta(y)}\frac{-\theta}{2\sqrt{1+\theta^2}}\Big(e^{i\sqrt{1+\theta^2}\tau}-e^{-i\sqrt{1+\theta^2}\tau}\Big)g(y)\,dy\,d\theta +$$

$$\frac{1}{2\pi}\int_{\mathbb{R}}\int_R e^{i\theta(\xi-y)}\frac{1}{2\sqrt{1+\theta^2}}\Big((1+\sqrt{1+\theta^2})e^{-i\sqrt{1+\theta^2}\tau}-(1-\sqrt{1+\theta^2})e^{i\sqrt{1+\theta^2}\tau}\Big)f(y)dyd\theta =$$

$$\frac{2i}{2\pi}\int_{\mathbb{R}}\Big[\int_{\mathbb{R}} e^{i\theta(\xi-y)}\frac{-\theta}{2\sqrt{1+\theta^2}}\sin\Big(\tau\sqrt{1+\theta^2}\Big)\,d\theta\Big]g(y)\,dy +$$

$$\frac{1}{2\pi}\int_{\mathbb{R}}\int_{\mathbb{R}} e^{i\theta(\xi-y)}\frac{1}{2\sqrt{1+\theta^2}}\Big[(1+\sqrt{1+\theta^2})e^{-i\sqrt{1+\theta^2}\tau}-(1-\sqrt{1+\theta^2})e^{i\sqrt{1+\theta^2}\tau}d\theta\Big]f(y)dy;$$

$$\psi_2(\xi,\tau) = \frac{1}{2\pi}\int_{\mathbb{R}} e^{i\theta x}\hat{\psi}_2(\theta,\tau)d\theta =$$

$$\frac{1}{2\pi}\int_{\mathbb{R}} e^{i\theta\xi}\Big((\frac{-1-\sqrt{1+\theta^2}}{\theta})(-\frac{\theta\hat{g}(\theta)+\hat{f}(\theta)(1-\sqrt{1+\theta^2})}{2\sqrt{1+\theta^2}})e^{i\sqrt{1+\theta^2}\tau}+$$

$$(\frac{-1+\sqrt{1+\theta^2}}{\theta})(\frac{\hat{g}(\theta)\theta+(1+\sqrt{1+\theta^2})\hat{f}(\theta)}{2\sqrt{1+\theta^2}})e^{-i\sqrt{1+\theta^2}\tau}\Big)d\theta =$$

$$\frac{1}{2\pi}\int_{\mathbb{R}} e^{i\theta\xi}\Big(\frac{1+\sqrt{1+\theta^2}}{\theta}\,\frac{\theta\hat{g}(\theta)+\hat{f}(\theta)(1-\sqrt{1+\theta^2})}{2\sqrt{1+\theta^2}}e^{i\sqrt{1+\theta^2}\tau}-$$

$$\frac{1-\sqrt{1+\theta^2}}{\theta}\,\frac{\theta\hat{g}(\theta)+\hat{f}(\theta)(1+\sqrt{1+\theta^2})}{2\sqrt{1+\theta^2}}e^{-i\sqrt{1+\theta^2}\tau}\Big)d\theta =$$

$$\frac{1}{2\pi}\int_{\mathbb{R}}\int_{\mathbb{R}} e^{i\theta(\xi-y)}\frac{1}{2\sqrt{1+\theta^2}}\Big[(1+\sqrt{1+\theta^2})e^{i\sqrt{1+\theta^2}\tau}-(1-\sqrt{1+\theta^2})e^{-i\sqrt{1+\theta^2}\tau}d\theta\Big]g(y)dy +$$

$$\frac{2i}{2\pi}\int_{\mathbb{R}}\Big[\int_{\mathbb{R}} e^{i\theta(\xi-y)}\frac{-\theta}{2\sqrt{1+\theta^2}}\sin\Big(\tau\sqrt{1+\theta^2}\Big)\,d\theta\Big]f(y)\,dy.$$

□

2.3. **Initial Boundary Value Problem.** In this section we solve initial boundary value problem of linear Dirac equation in (1+1) dimension for $\xi \in [0,1]$ and $\tau \in [0,\pi/2]$. The method that we use is separation of variables.

Theorem 2.3. *Let f and g be functions defined on the interval $[0,1]$ satisfying that $f(0) = f(1)$, $g(0) = g(1)$. Assume also that they can be expanded as Fourier series by*

$$f(\xi) = \sum_{n=-\infty}^{\infty} f_n e^{2i\pi n\xi}, \quad g(\xi) = \sum_{n=-\infty}^{\infty} g_n e^{2i\pi n\xi},$$

where

$$f_0 = \int_0^1 f(\xi)\,d\xi = 0, \quad g_0 = \int_0^1 g(\xi)\,d\xi = 0$$

and

$$f_n = \int_0^1 f(\xi)\,e^{2\pi in\xi}d\xi, \quad g_n = \int_0^1 g(\xi)\,e^{2i\pi n\xi}\,d\xi, \quad n \in \mathbb{Z}.$$

Then the linear Dirac equation in (1+1) dimension for any $\xi \in [0,1]$ and $\tau \in [0,\pi/2]$

$$\begin{cases} \partial_\tau\psi_1(\xi,\tau) + \partial_\xi\psi_2(\xi,\tau) + i\psi_1(\xi,\tau) = 0 \\ -\partial_\tau\psi_2(\xi,\tau) - \partial_\xi\psi_1(\xi,\tau) + i\psi_2(\xi,\tau) = 0, \\ \psi_1(\xi,0) = f(\xi), \\ \psi_2(\xi,0) = g(\xi), \\ \psi_1(0,\tau) = \psi_1(1,\tau) \\ \psi_2(0,\tau) = \psi_2(1,\tau) \end{cases}$$

has for solution

$$\begin{pmatrix} \psi_1(\xi,\tau) \\ \psi_2(\xi,\tau) \end{pmatrix} = \sum_{n\in\mathbb{N}}\Big(\sum_{j=1}^{4} C_n^j\Psi_{n,1}^j(\xi,\tau) + D_n^j\Psi_{n,2}^j(\xi,\tau)\Big)$$

where the constants C_n^j and D_n^j satisfy the relations

$$C_n^1 + C_n^2 = \frac{f_n\alpha_n^{-1} - g_n}{\alpha_n + \alpha_n^{-1}}, \quad C_n^3 + C_n^4 = \frac{g_n + \alpha_n f_n}{\alpha_n + \alpha_n^{-1}},$$

$$D_n^1 + D_n^2 = \frac{g_{-n} + \alpha_n^{-1}f_{-n}}{\alpha_n + \alpha_n^{-1}}, \quad D_n^3 + D_n^4 = \frac{\alpha_n f_{-n} - g_{-n}}{\alpha_n + \alpha_n^{-1}}$$

for

$$\alpha_n = \sqrt{\frac{\sqrt{4\pi^2n^2+1}+1}{\sqrt{4\pi^2n^2+1}-1}}$$

and

$$\Psi_{n,1}^1(\xi,\tau) = \begin{pmatrix} 1 \\ -\alpha_n \end{pmatrix} e^{2i\pi n\xi}e^{i\sqrt{4\pi^2n^2+1}\tau}, \quad \Psi_{n,1}^2 = \begin{pmatrix} 1 \\ -\alpha_n \end{pmatrix} e^{2i\pi n\xi}e^{-i\sqrt{4\pi^2n^2+1}\tau}$$

$$\Psi_{n,1}^3(\xi,\tau) = \begin{pmatrix} 1 \\ \alpha_n^{-1} \end{pmatrix} e^{2i\pi n\xi}e^{i\sqrt{4\pi^2n^2+1}\tau}, \quad \Psi_{n,1}^4 = \begin{pmatrix} 1 \\ \alpha_n^{-1} \end{pmatrix} e^{2i\pi n\xi}e^{-i\sqrt{4\pi^2n^2+1}\tau}$$

$$\Psi_{n,2}^1(\xi,\tau) = \begin{pmatrix} 1 \\ \alpha_n \end{pmatrix} e^{-2i\pi n\xi}e^{i\sqrt{4\pi^2n^2+1}\tau}, \quad \Psi_{n,2}^2 = \begin{pmatrix} 1 \\ \alpha_n \end{pmatrix} e^{-2i\pi n\xi}e^{-i\sqrt{4\pi^2n^2+1}\tau}$$

$$\Psi^3_{n,2}(\xi,\tau) = \begin{pmatrix} 1 \\ -\alpha_n^{-1} \end{pmatrix} e^{-2i\pi n\xi} e^{i\sqrt{4\pi^2n^2+1}\tau}, \quad \Psi^4_{n,2} = \begin{pmatrix} 1 \\ -\alpha_n^{-1} \end{pmatrix} e^{-2i\pi n\xi} e^{-i\sqrt{4\pi^2n^2+1}\tau}$$

Proof. To solve initial boundary value problem we use method separation of variables which is the following:

$$\psi(x,t) = \chi(\xi)T(\tau) = \chi(\xi)e^{iE\tau}$$

For convenience let's divide proof to several steps:

Step 1: Substitution of $\psi(x,t) = \chi(\xi)T(\tau) = \chi(\xi)e^{iE\tau}$ to (6):

$$\begin{bmatrix} iE\chi_1(\xi)e^{iE\tau} \\ -iE\chi_2(\xi)e^{iE\tau} \end{bmatrix} + \begin{bmatrix} \chi_2'(\xi)e^{iE\tau} \\ -\chi_1'(\xi)e^{iE\tau} \end{bmatrix} + i\begin{bmatrix} \chi_1(\xi)e^{iE\tau} \\ \chi_2(\xi)e^{iE\tau} \end{bmatrix} = \begin{bmatrix} 0 \\ 0 \end{bmatrix}.$$

Step 2: Division by $e^{iE\tau}$ and rewriting as follows:

$$\begin{bmatrix} \chi_1'(\xi) \\ -\chi_2'(\xi) \end{bmatrix} + \begin{bmatrix} iE\chi_2(\xi) \\ -iE\chi_1(\xi) \end{bmatrix} + i\begin{bmatrix} \chi_1(\xi) \\ \chi_2(\xi) \end{bmatrix} = 0.$$

Thus, we obtain system of ordinary differential equations in $\chi(\xi)$:

$$\begin{bmatrix} \chi_1'(\xi) \\ \chi_2'(\xi) \end{bmatrix} = \begin{bmatrix} 0 & -i(E-1) \\ -i(E+1) & 0 \end{bmatrix} \begin{bmatrix} \chi_1(\xi) \\ \chi_2(\xi) \end{bmatrix}. \tag{17}$$

In our system of ordinary differential equations we have a constant E that we need to consider with the following three cases:

(1) $E = 1$
(2) $E > 1$
(3) $E < 1$

Let's begin with the first case when $E = 1$:

Step 3 Substitution of $E = 1$ to (17) leads to trivial solutions which is not interesting for us

$$\begin{bmatrix} \chi_1'(\xi) \\ \chi_2'(\xi) \end{bmatrix} = \begin{bmatrix} 0 & 0 \\ -2i & 0 \end{bmatrix} \begin{bmatrix} \chi_1(\xi) \\ \chi_2(\xi) \end{bmatrix}.$$

Step 4: Now let's proceed with the second case $E > 1$:

$$\begin{bmatrix} \chi_1'(\xi) \\ \chi_2'(\xi) \end{bmatrix} = \begin{bmatrix} 0 & -i(E-1) \\ -i(E+1) & 0 \end{bmatrix} \begin{bmatrix} \chi_1(\xi) \\ \chi_2(\xi) \end{bmatrix}.$$

To find solutions explicitly we assume that $\chi(\xi) = \eta e^{rt}$ and substitute for χ and obtain system of algebraic equations [3]:

$$\begin{bmatrix} -r & -i(E-1) \\ -i(E+1) & -r \end{bmatrix} \begin{bmatrix} \eta_1 \\ \eta_2 \end{bmatrix} = \begin{bmatrix} 0 \\ 0 \end{bmatrix}.$$

Acceptable values of r are as follows: $r_{1,2} = \pm i\sqrt{E^2-1}$ which are eigenvalues of our system. Now let's find corresponding eigenvectors

Case r_1 :

$$\begin{bmatrix} -i\sqrt{E^2-1} & -i(E-1) \\ -i(E+1) & -i\sqrt{E^2-1} \end{bmatrix} \begin{bmatrix} \eta_1^{(1)} \\ \eta_2^{(1)} \end{bmatrix} = \begin{bmatrix} 0 \\ 0 \end{bmatrix}.$$

which results in $\eta_1^{(1)} = 1, \eta_2^{(1)} = -\frac{\sqrt{E+1}}{\sqrt{E-1}}$ and $\eta_1^{(2)} = 1, \eta_2^{(2)} = \frac{\sqrt{E+1}}{\sqrt{E-1}}$:

$$\chi_1(\xi) = \begin{pmatrix} 1 \\ -\frac{\sqrt{E+1}}{\sqrt{E-1}} \end{pmatrix} e^{i\sqrt{E^2-1}\xi}, \quad \chi_2(\xi) = \begin{pmatrix} 1 \\ \frac{\sqrt{E+1}}{\sqrt{E-1}} \end{pmatrix} e^{-i\sqrt{E^2-1}\xi}.$$

The solutions χ_1 and χ_2 form a fundamental set, and the general solution of the system is

$$\chi = C\chi^{(1)}(\xi) + D\chi^{(2)}(\xi) = C\begin{pmatrix} 1 \\ -\frac{\sqrt{E+1}}{\sqrt{E-1}} \end{pmatrix} e^{i\sqrt{E^2-1}\xi} + D\begin{pmatrix} 1 \\ \frac{\sqrt{E+1}}{\sqrt{E-1}} \end{pmatrix} e^{-i\sqrt{E^2-1}\xi},$$

where C and D are arbitrary constants.

Step 5: Now let's apply periodic boundary conditions to find out $E:$

$$\begin{cases} \chi_1(0) = \chi_1(1), \\ \chi_2(0) = \chi_2(1) \end{cases}$$

which results in the following system:

$$\begin{cases} C + D = Ce^{i\sqrt{E^2-1}} + De^{-i\sqrt{E^2-1}}, \\ -C\frac{\sqrt{E+1}}{\sqrt{E-1}} + D\frac{\sqrt{E+1}}{\sqrt{E-1}} = -C\frac{\sqrt{E+1}}{\sqrt{E-1}}e^{i\sqrt{E^2-1}} + D\frac{\sqrt{E+1}}{\sqrt{E-1}}e^{-i\sqrt{E^2-1}}. \end{cases}$$

System leads to following equation where we can obtain value of of E,

$$2C\left(1 - e^{i\sqrt{E^2-1}}\right) = 0,$$

which is the following:

$$E = \pm\sqrt{4\pi^2 n^2 + 1}.$$

Step 6: We can begin with the substitution of positive value of $E:$

$$\begin{cases} \psi_1(\xi,\tau) = C_n^1 e^{2i\pi n\xi} e^{i\sqrt{4\pi^2n^2+1}\tau} + D_n^1 e^{-2i\pi n\xi} e^{i\sqrt{4\pi^2n^2+1}\tau}, \\ \psi_2(\xi,\tau) = \left(\frac{\sqrt{\sqrt{4\pi^2n^2+1}+1}}{\sqrt{\sqrt{4\pi^2n^2+1}-1}}\right)\left(-C_n^1 e^{2i\pi n\xi} e^{i\sqrt{4\pi^2n^2+1}\tau} + D_n^1 e^{-2i\pi n\xi} e^{i\sqrt{4\pi^2n^2+1}\tau}\right) \end{cases}$$

and as for the negative value of E we obtain the following system:

$$\begin{cases} \psi_1(\xi,\tau) = C_n^2 e^{2i\pi n\xi} e^{-i\sqrt{4\pi^2n^2+1}\tau} + D_n^2 e^{-2i\pi n\xi} e^{-i\sqrt{4\pi^2n^2+1}\tau}, \\ \psi_2(\xi,\tau) = \frac{\sqrt{\sqrt{4\pi^2n^2+1}+1}}{\sqrt{\sqrt{4\pi^2n^2+1}-1}}\left(-C_n^2 e^{2i\pi n\xi} e^{-i\sqrt{4\pi^2n^2+1}\tau} + D_n^2 e^{-2i\pi n\xi} e^{-i\sqrt{4\pi^2n^2+1}\tau}\right) \end{cases}$$

Step 7: $\mathbf{E < 1}$**:** For this case we follow the idea of case $E > 1$ and obtain two eigenvalues which are as follows: $r_{1,2} = \pm i\sqrt{E^2-1}$. Therefore our corresponding eigenvectors are: $\eta_1^{(1)} = 1, \eta_2^{(1)} = \frac{\sqrt{E-1}}{\sqrt{E+1}}$ and $\eta_1^{(2)} = 1, \eta_2^{(2)} = -\frac{\sqrt{E-1}}{\sqrt{E+1}}$. Thus, the solution in $\chi_1(\xi)$ and $\chi_2(\xi)$ are:

$$\chi_1(\xi) = \begin{pmatrix} 1 \\ \frac{\sqrt{E-1}}{\sqrt{E+1}} \end{pmatrix} e^{i\sqrt{E^2-1}\xi}, \quad \chi_2(\xi) = \begin{pmatrix} 1 \\ -\frac{\sqrt{E-1}}{\sqrt{E+1}} \end{pmatrix} e^{-i\sqrt{E^2-1}\xi}.$$

The solutions χ_1 and χ_2 form a fundamental set, and the general solution of the system is

$$\chi = C\chi_1(\xi) + D\chi_2\xi) = C\begin{pmatrix} 1 \\ \frac{\sqrt{E-1}}{\sqrt{E+1}} \end{pmatrix} e^{i\sqrt{E^2-1}\xi} + D\begin{pmatrix} 1 \\ -\frac{\sqrt{E-1}}{\sqrt{E+1}} \end{pmatrix} e^{-i\sqrt{E^2-1}\xi},$$

where C and D are arbitrary constants.

Step 8: Our next aim is to find out constant E and we apply periodic boundary conditions:

$$\begin{cases} \chi_1(0) = \chi_1(1), \\ \chi_2(0) = \chi_2(1) \end{cases}$$

which results in the following system of equations:

$$\begin{cases} C + D = Ce^{i\sqrt{E^2-1}} + De^{-i\sqrt{E^2-1}}, \\ C\frac{\sqrt{E-1}}{\sqrt{E+1}} - D\frac{\sqrt{E-1}}{\sqrt{E+1}} = C\frac{\sqrt{E-1}}{\sqrt{E+1}}e^{i\sqrt{E^2-1}} - D\frac{\sqrt{E-1}}{\sqrt{E+1}}e^{-i\sqrt{E^2-1}}. \end{cases}$$

Solving the system leads to:

$$2C\Big(1 - e^{i\sqrt{E^2-1}}\Big) = 0,$$

where follows that $E = \pm\sqrt{4\pi^2 n^2 + 1}$.

Since we have found constant E, we can start with its positive value:

$$\begin{cases} \psi_1(\xi,\tau) = C_n^3 e^{2i\pi n\xi} e^{i\sqrt{4\pi^2n^2+1}\tau} + D_n^3 e^{-2i\pi n\xi} e^{i\sqrt{4\pi^2n^2+1}\tau}, \\ \psi_2(\xi,\tau) = \frac{\sqrt{\sqrt{4\pi^2n^2+1}-1}}{\sqrt{\sqrt{4\pi^2n^2+1}+1}}\left(C_n^3 e^{2i\pi n\xi} e^{i\sqrt{4\pi^2n^2+1}\tau} - D_n^3 e^{-2i\pi n\xi} e^{i\sqrt{4\pi^2n^2+1}\tau}\right) \end{cases}$$

As for the negative value of E we get:

$$\begin{cases} \psi_1(\xi,\tau) = C_n^4 e^{2i\pi n\xi} e^{-i\sqrt{4\pi^2n^2+1}\tau} + D_n^4 e^{-2i\pi n\xi} e^{-i\sqrt{4\pi^2n^2+1}\tau}, \\ \psi_2(\xi,\tau) = \frac{\sqrt{\sqrt{4\pi^2n^2+1}-1}}{\sqrt{\sqrt{4\pi^2n^2+1}+1}}\left(C_n^4 e^{2i\pi n\xi} e^{-i\sqrt{4\pi^2n^2+1}\tau} - D_n^4 e^{-2i\pi n\xi} e^{-i\sqrt{4\pi^2n^2+1}\tau}\right) \end{cases}$$

In conclusion, we found that for each $n \in \mathbb{N}$ and any constants C_n^j, D_n^j, $j = 1,2,3,4$, the following is a solution of our system of PDEs together with our boundary conditions

$$\Psi_n(\xi,\tau) = \sum_{j=1}^{4} C_n^j \Psi_{n,1}^j(\xi,\tau) + D_n^j \Psi_{n,2}^j(\xi,\tau).$$

Moreover, since our problem is linear, the following is also a solution of our system of PDEs together with our boundary conditions

$$\Psi(\xi,\tau) = \sum_{n\in\mathbb{N}} \Psi_n(\xi,\tau) = \sum_{n\in\mathbb{N}} \Big(\sum_{j=1}^{4} C_n^j \Psi_{n,1}^j(\xi,\tau) + D_n^j \Psi_{n,2}^j(\xi,\tau)\Big).$$

Now, given an initial data

$$F(\xi) = \begin{pmatrix} f(\xi) \\ g(\xi) \end{pmatrix},$$

we need to find constants C_n^j, D_n^j, $j = 1,2,3,4$, such that

$$F(\xi) = \Psi(\xi,0). \tag{18}$$

Define,

$$\alpha_n := \frac{\sqrt{\sqrt{4\pi^2n^2+1}+1}}{\sqrt{\sqrt{4\pi^2n^2+1}-1}}$$

From above computations we have that,

$$\begin{aligned} \Psi(\xi,0) = &\sum_{n\in\mathbb{N}} \Big[C_n^1 \begin{pmatrix} 1 \\ -\alpha_n \end{pmatrix} e^{2i\pi n\xi} + D_n^1 \begin{pmatrix} 1 \\ \alpha_n \end{pmatrix} e^{-2i\pi n\xi}\Big] \\ &+ \sum_{n\in\mathbb{N}} \Big[C_n^2 \begin{pmatrix} 1 \\ -\alpha_n \end{pmatrix} e^{2i\pi n\xi} + D_n^2 \begin{pmatrix} 1 \\ \alpha_n \end{pmatrix} e^{-2i\pi n\xi}\Big] \\ &+ \sum_{n\in\mathbb{N}} \Big[C_n^3 \begin{pmatrix} 1 \\ \alpha_n^{-1} \end{pmatrix} e^{2i\pi n\xi} + D_n^3 \begin{pmatrix} 1 \\ -\alpha_n^{-1} \end{pmatrix} e^{-2i\pi n\xi}\Big] \\ &+ \sum_{n\in\mathbb{N}} \Big[C_n^4 \begin{pmatrix} 1 \\ \alpha_n^{-1} \end{pmatrix} e^{2i\pi n\xi} + D_n^4 \begin{pmatrix} 1 \\ -\alpha_n^{-1} \end{pmatrix} e^{-2i\pi n\xi}\Big] \qquad (19) \\ = &\sum_{n\in\mathbb{N}} \Big[\Big(C_n^1 \begin{pmatrix} 1 \\ -\alpha_n \end{pmatrix} + C_n^2 \begin{pmatrix} 1 \\ -\alpha_n \end{pmatrix} + C_n^3 \begin{pmatrix} 1 \\ \alpha_n^{-1} \end{pmatrix} + C_n^4 \begin{pmatrix} 1 \\ \alpha_n^{-1} \end{pmatrix}\Big) e^{2i\pi n\xi} \end{aligned}$$

$$+\left(D_n^1\begin{pmatrix}1\\ \alpha_n\end{pmatrix}+D_n^2\begin{pmatrix}1\\ \alpha_n\end{pmatrix}+D_n^3\begin{pmatrix}1\\ -\alpha_n^{-1}\end{pmatrix}+D_n^4\begin{pmatrix}1\\ -\alpha_n^{-1}\end{pmatrix}\right)e^{-2i\pi n\xi}\Bigg]$$

$$=\sum_{n=1}^{\infty}\Bigg[\left((C_n^1+C_n^2)\begin{pmatrix}1\\ -\alpha_n\end{pmatrix}+(C_n^3+C_n^4)\begin{pmatrix}1\\ \alpha_n^{-1}\end{pmatrix}\right)e^{2i\pi n\xi}$$

$$+\left((D_n^1+D_n^2)\begin{pmatrix}1\\ \alpha_n\end{pmatrix}+(D_n^3+D_n^4)\begin{pmatrix}1\\ -\alpha_n^{-1}\end{pmatrix}\right)e^{-2i\pi n\xi}\Bigg]$$

We can assume that

$$\begin{aligned} f(\xi)&=\sum_{n\in\mathbb{Z}}f_ne^{2i\pi n\xi}=\sum_{n=-1}^{\infty}f_ne^{2i\pi n\xi}+f_0+\sum_{n=1}^{\infty}f_ne^{2i\pi n\xi}\\ &=\sum_{n=1}^{\infty}f_{-n}e^{-2i\pi n\xi}+f_0+\sum_{n=1}^{\infty}f_ne^{2i\pi n\xi}\end{aligned}$$

and

$$g(\xi)=\sum_{n\in\mathbb{Z}}g_ne^{2i\pi n\xi}=\sum_{n=1}^{\infty}g_{-n}e^{-2i\pi n\xi}+g_0+\sum_{n=1}^{\infty}g_ne^{2i\pi n\xi}.$$

Step 9: Finding constants from the system:

$$\begin{cases} C_n^1+C_n^2+C_n^3+C_n^4=f_n\\ -\alpha_n(C_n^1+C_n^2)+\alpha_n^{-1}(C_n^3+C_n^4)=g_n\\ D_n^1+D_n^2+D_n^3+D_n^4=f_{-n}\\ \alpha_n(D_n^1+D_n^2)-\alpha_n^{-1}(D_n^3+D_n^4)=g_{-n}\end{cases}$$

$$C_n^1+C_n^2=\frac{f_n\alpha_n^{-1}-g_n}{\alpha_n+\alpha_n^{-1}},\quad C_n^3+C_n^4=\frac{g_n+\alpha_nf_n}{\alpha_n+\alpha_n^{-1}},$$

$$D_n^1+D_n^2=\frac{g_{-n}+\alpha_n^{-1}f_{-n}}{\alpha_n+\alpha_n^{-1}},\quad D_n^3+D_n^4=\frac{\alpha_nf_{-n}-g_{-n}}{\alpha_n+\alpha_n^{-1}}$$

□

2.3.1. *Example 1.*

Example 1. *Let's consider following problem for any* $\xi\in[0,1]$ *and* $\tau\in[0,\pi/2]$ *:*

$$\begin{cases}\partial_\tau\psi_1(\xi,\tau)+\partial_\xi\psi_2(\xi,\tau)+i\psi_1(\xi,\tau)=0,\\ -\partial_\tau\psi_2(\xi,\tau)-\partial_\xi\psi_1(\xi,\tau)+i\psi_2(\xi,\tau)=0,\\ \psi_1(\xi,0)=e^{2i\pi\xi},\\ \psi_2(\xi,0)=-\frac{\sqrt{\sqrt{4\pi^2+1}+1}}{\sqrt{\sqrt{4\pi^2+1}-1}}e^{2i\pi\xi},\\ \psi_1(0,\tau)=\psi_1(1,\tau),\\ \psi_2(0,\tau)=\psi_2(1,\tau).\end{cases}\tag{20}$$

which has for solution:

$$\begin{cases}\psi_1(\xi,\tau)=e^{2i\pi x}e^{i\sqrt{4\pi^2+1}\tau},\\ \psi_2(\xi,\tau)=-\frac{\sqrt{\sqrt{4\pi^2+1}+1}}{\sqrt{\sqrt{4\pi^2+1}-1}}e^{2i\pi\xi}e^{i\sqrt{4\pi^2+1}\tau}.\end{cases}$$

Observe that, indeed this example is a particular case of Theorem 2.3 taken with

$$f(\xi)=e^{2i\pi\xi}\quad\text{and}\quad g(\xi)=-\sqrt{\frac{\sqrt{4\pi^2+1}+1}{\sqrt{4\pi^2+1}-1}}e^{2i\pi\xi}.$$

Moreover, its solution can be obtained using Lemma 2.1 applying specific parameters:

$$k = 2\pi, \quad \omega = \sqrt{4\pi^2+1}, \quad a_1 = 1 \quad \text{and} \quad 2 = -\sqrt{\frac{\sqrt{4\pi^2+1}+1}{\sqrt{4\pi^2+1}-1}}.$$

Note that our PDE (20) is complex and we can separate it to real and imaginary parts

$$\begin{cases} \psi_1(\xi,\tau) = u_1(\xi,\tau) + iv_1(\xi,\tau), \\ \psi_2(\xi,\tau) = u_2(\xi,\tau) + iv_2(\xi,\tau) \end{cases}$$

which leads to following problem

$$\begin{cases} \partial_\tau u_1(\xi,\tau) + \partial_\xi u_2(\xi,\tau) - v_1(\xi,\tau) = 0, \\ \partial_\tau v_1(\xi,\tau) + \partial_\xi v_2(\xi,\tau) + u_1(\xi,\tau) = 0, \\ -\partial_\tau u_2(\xi,\tau) - \partial_\xi u_1(\xi,\tau) - v_2(\xi,\tau) = 0, \\ -\partial_\tau v_2(\xi,\tau) - \partial_\xi v_1(\xi,\tau) + u_2(\xi,\tau) = 0, \\ u_1(\xi,0) = \cos(2\pi\xi), \\ v_1(\xi,0) = \sin(2\pi\xi), \\ u_2(\xi,0) = -\frac{\sqrt{\sqrt{4\pi^2+1}+1}}{\sqrt{\sqrt{4\pi^2+1}-1}}\cos(2\pi\xi), \\ v_2(\xi,0) = -\frac{\sqrt{\sqrt{4\pi^2+1}+1}}{\sqrt{\sqrt{4\pi^2+1}-1}}\sin(2\pi\xi), \\ u_1(0,\tau) = u_1(1,\tau), \\ v_1(0,\tau) = v_1(1,\tau), \\ u_2(0,\tau) = u_2(1,\tau), \\ v_2(0,\tau) = v_2(1,\tau), \end{cases} \tag{21}$$

and corresponding solution is:

$$\begin{cases} u_1(\xi,\tau) = \cos\left(2\pi\xi + \sqrt{4\pi^2+1}\tau\right), \\ v_1(\xi,\tau) = \sin\left(2\pi\xi + \sqrt{4\pi^2+1}\tau\right), \\ u_2(\xi,\tau) = -\sqrt{\frac{\sqrt{4\pi^2+1}+1}{\sqrt{4\pi^2+1}-1}}\cos\left(2\pi\xi + \sqrt{4\pi^2+1}\tau\right), \\ v_2(\xi,\tau) = -\sqrt{\frac{\sqrt{4\pi^2+1}+1}{\sqrt{4\pi^2+1}-1}}\sin\left(2\pi\xi + \sqrt{4\pi^2+1}\tau\right). \end{cases}$$

Observe that we converted the original system of 2 unknowns to a system of 4 unknowns which are $u_1(\xi,\tau), v_1(\xi,\tau), u_2(\xi,\tau)$ and $v_2(\xi,\tau)$.

Below are illustrated graphs of $u_1(\xi,\tau), v_1(\xi,\tau), u_2(\xi,\tau)$ and $v_2(\xi,\tau)$ for $\xi \in [0,1]$ and $\tau_1 = 0, \tau_2 = \pi/8 \sim 0.39, \tau_3 = \pi/4 \sim 0.79,\ \tau_4 = \pi/2 \sim 1.57$.

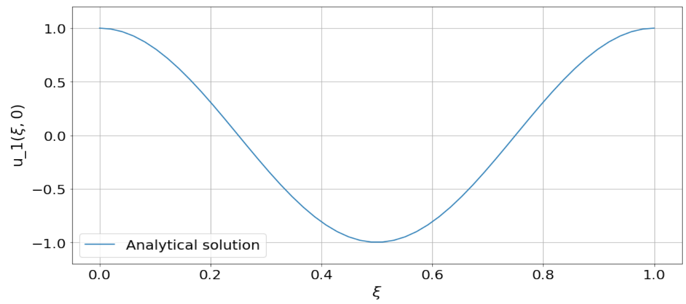

FIGURE 1. Graph of $u_1(\xi, 0)$

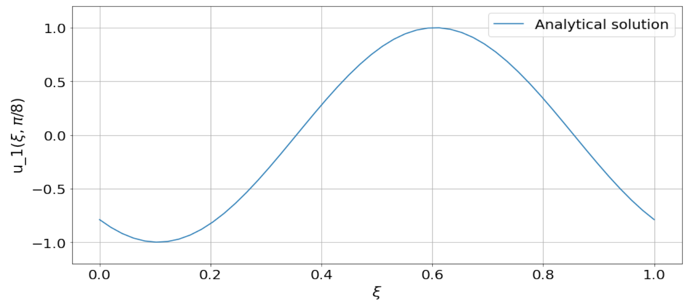

FIGURE 2. Graph of $u_1(\xi, 0.39)$

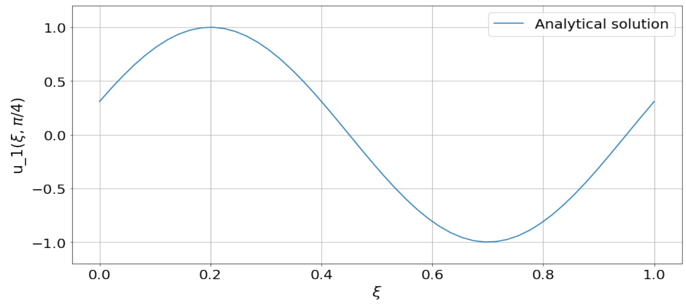

FIGURE 3. Graph of $u_1(\xi, 0.79)$

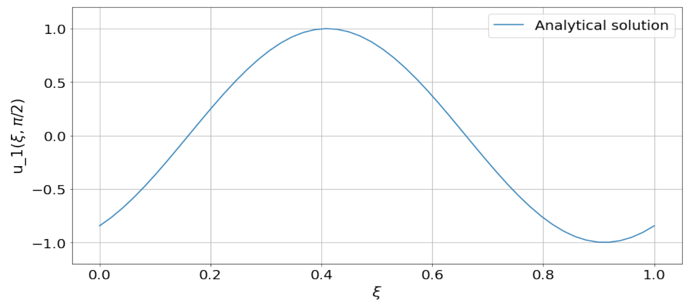

FIGURE 4. Graph of $u_1(\xi, 1.57)$

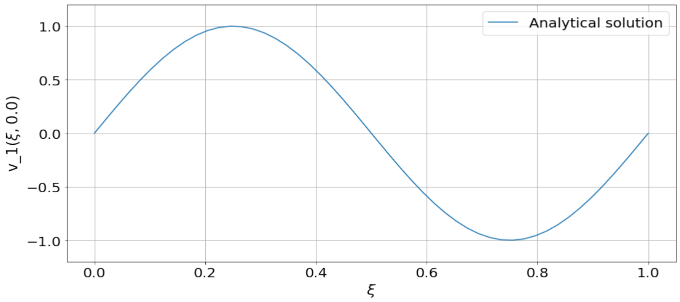

FIGURE 5. Graph of $v_1(\xi, 0)$

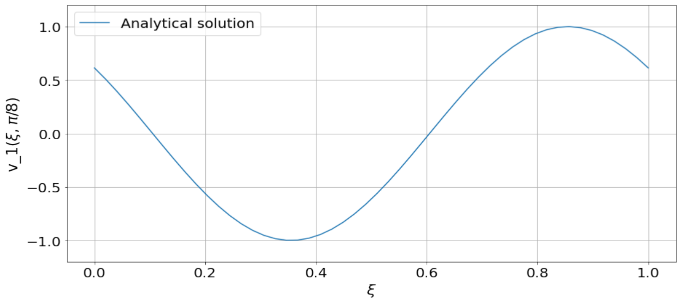

FIGURE 6. Graph of $v_1(\xi, 0.39)$

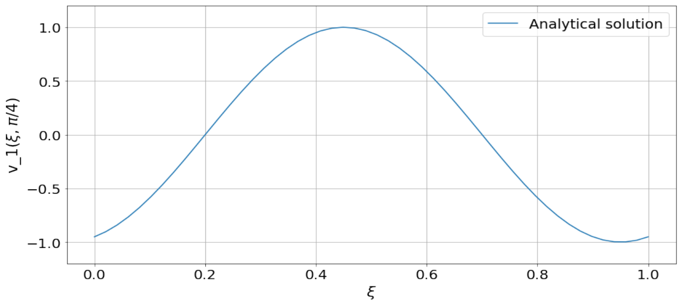

FIGURE 7. Graph of $v_1(\xi, 0.79)$

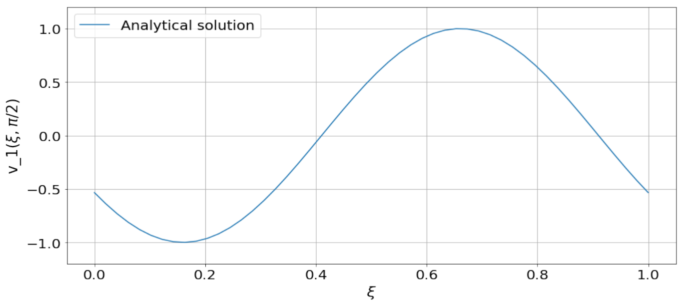

FIGURE 8. Graph of $v_1(\xi, 1.57)$

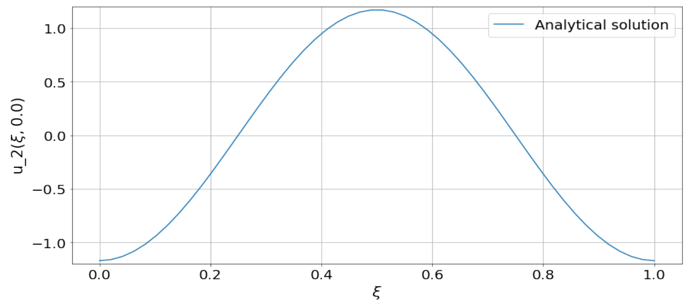

FIGURE 9. Graph of $u_2(\xi, 0)$

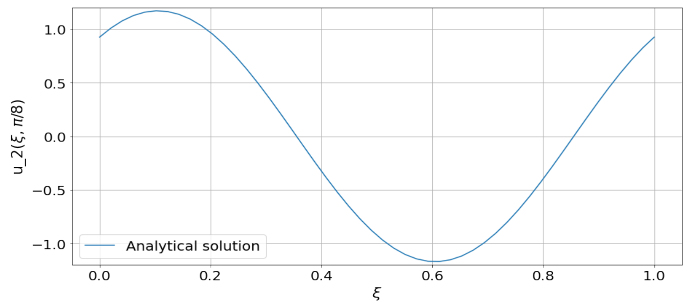

FIGURE 10. Graph of $u_2(\xi, 0.39)$

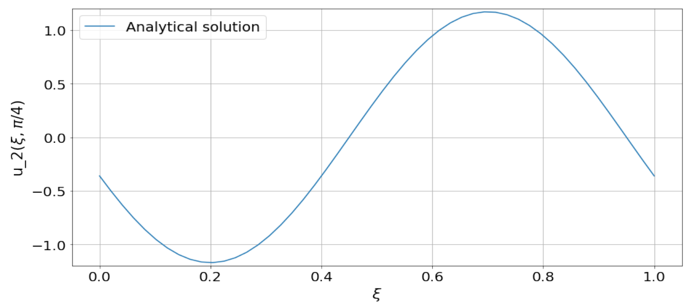

FIGURE 11. Graph of $u_2(\xi, 0.79)$

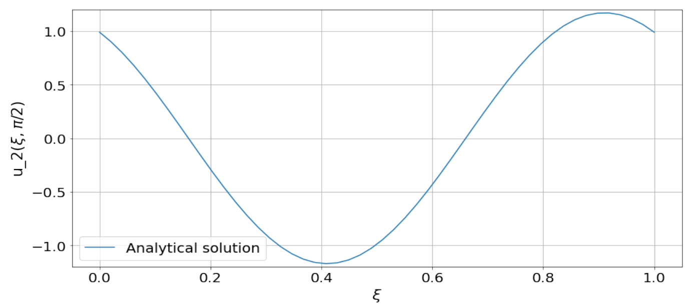

FIGURE 12. Graph of $u_2(\xi, 1.57)$

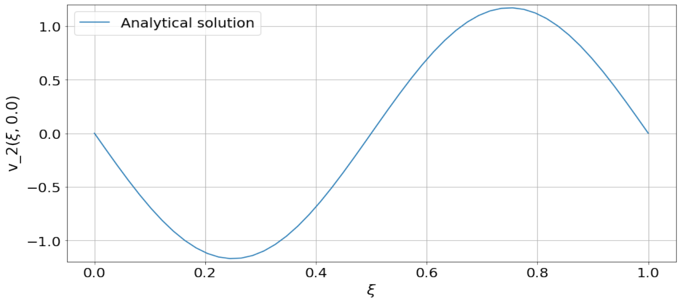

FIGURE 13. Graph of $v_2(\xi, 0)$

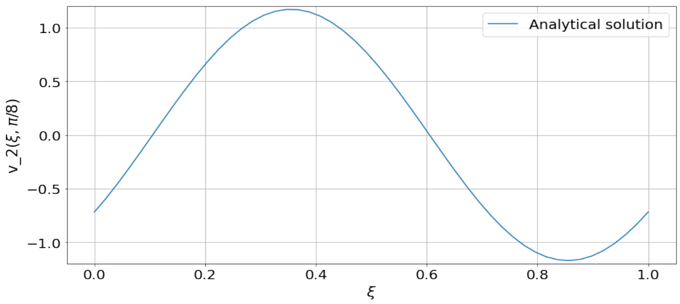

FIGURE 14. Graph of $v_2(\xi, 0.39)$

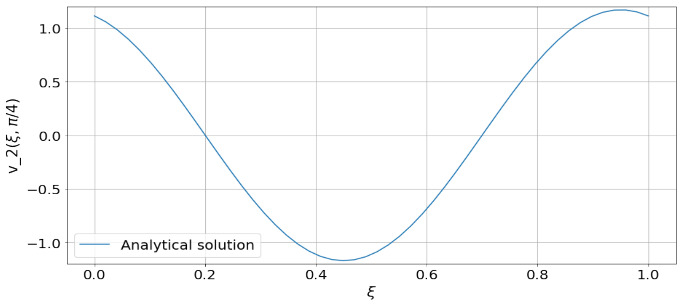

FIGURE 15. Graph of $v_2(\xi, 0.79)$

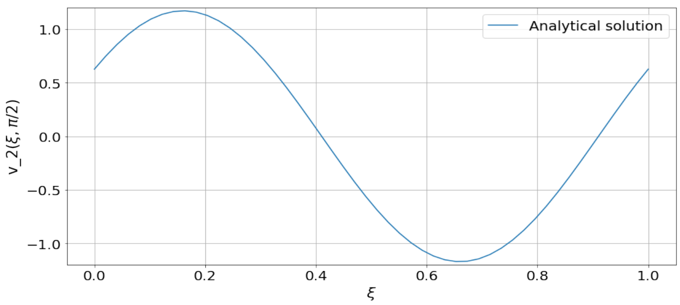

FIGURE 16. Graph of $v_2(\xi, 1.57)$

2.3.2. *Example 2.*

Example 2. *Consider following problem*

$$\begin{cases} \partial_\tau \psi_1(\xi,\tau) + \partial_\xi \psi_2(\xi,\tau) + i\psi_1(\xi,\tau) = 0 \\ -\partial_\tau \psi_2(\xi,\tau) - \partial_\xi \psi_1(\xi,\tau) + i\psi_2(\xi,\tau) = 0, \\ \psi_1(\xi,0) = \xi^2 - \xi + \frac{1}{6}, \\ \psi_2(\xi,0) = \begin{cases} \xi - 0.25, & 0 \le \xi \le 1/2 \\ -\xi + 0.75, & 1/2 \le \xi \le 1 \end{cases} \\ \psi_1(0,\tau) = \psi_1(1,\tau) \\ \psi_2(0,\tau) = \psi_2(1,\tau) \end{cases}$$

Note that the solution can be obtained as an application of Theorem 2.3, with

$$f(\xi) = \xi^2 - \xi + 1/6, \quad g(\xi) = \begin{cases} \xi - 0.25 & 0 < \xi < 0.5, \\ -\xi + 0.75 & 0.5 < \xi < 1 \end{cases}$$

and corresponding Fourier coefficients

$$f_n = \frac{2i(e^{2i\pi n} - 1)(3 - \pi^2 n^2) + 6\pi n(e^{2i\pi n} + 1)}{24\pi^3 n^3}, \tag{22}$$

$$g_n = \frac{(e^{2i\pi n} - 1)i\pi n - 2(e^{2i\pi n} + 1) + 4e^{i\pi n}}{8\pi^2 n^2} \tag{23}$$

For future neural network approximation we need to truncate the Fourier series as follows

$$f(\xi) = \sum_{n=-N}^{N} f_n e^{2i\pi n\xi}$$

and

$$g(\xi) = \sum_{n=-N}^{N} g_n e^{2i\pi n\xi},$$

for some convenient $N \in \mathbb{N}$.

Let's begin with $N = 10$:

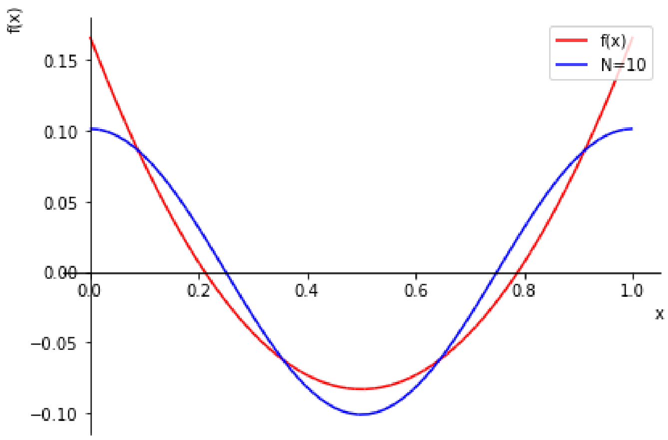

FIGURE 17. Truncating Fourier Series of f

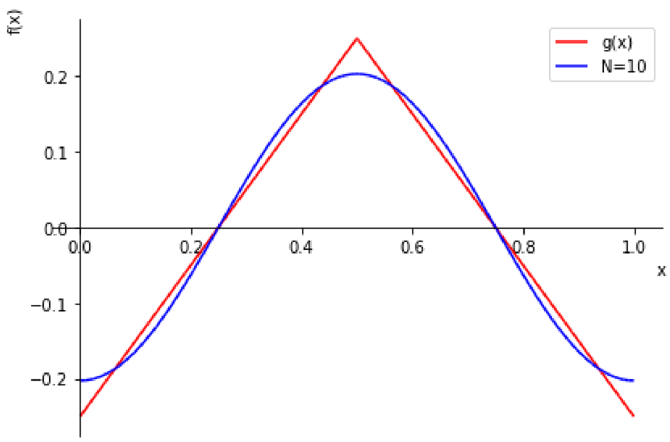

FIGURE 18. Truncating Fourier Series of g

According to the obtained graphs we see that we need to add more terms to the truncation.

Let's experiment with $N = 30$:

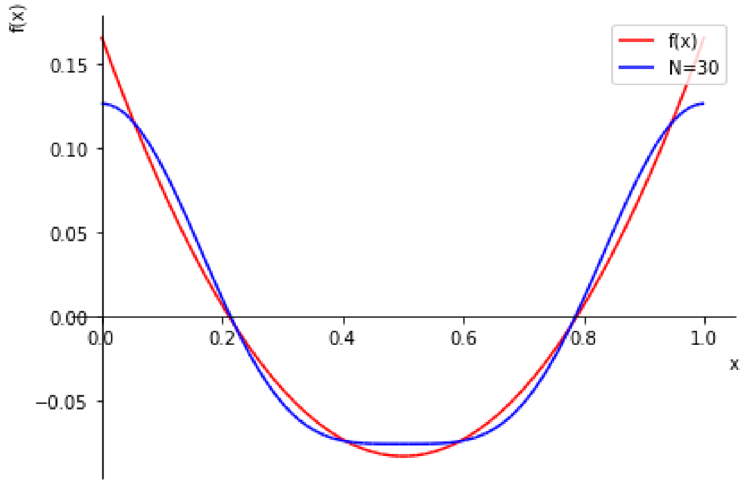

FIGURE 19. Truncating Fourier Series f

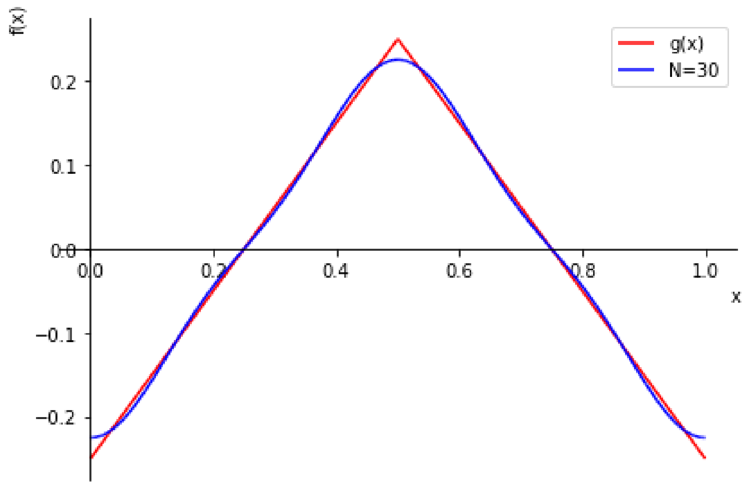

FIGURE 20. Truncating Fourier Series g

Observe that our approximation needs even more terms in the truncation.

Let's take now $N = 80$:

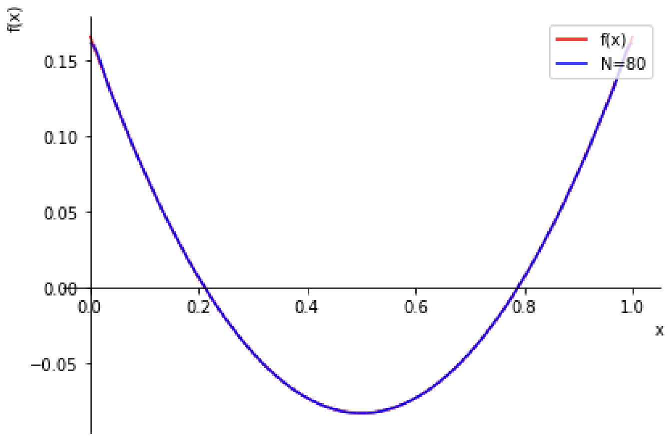

FIGURE 21. Truncating Fourier Series f

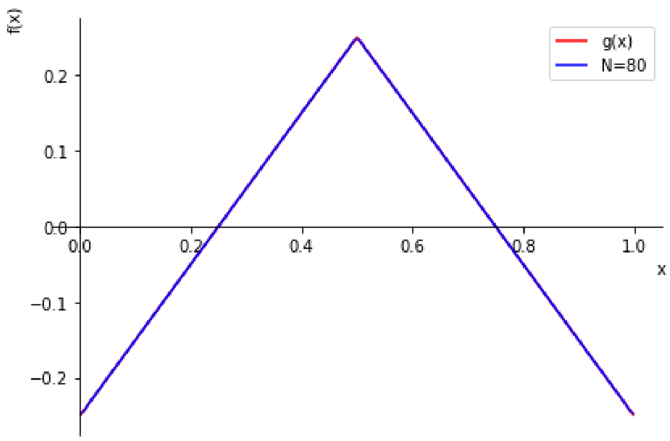

FIGURE 22. Truncating Fourier Series g

Since our PDE is complex, we can separate it to real and imaginary parts:

$$\begin{cases}\psi_1(\xi,\tau) = u_1(\xi,\tau) + iv_1(\xi,\tau),\\ \psi_2(\xi,\tau) = u_2(\xi,\tau) + iv_2(\xi,\tau),\end{cases}$$

which leads to following problem:

$$\begin{cases}\partial_\tau u_1(\xi,\tau) + \partial_\xi u_2(\xi,\tau) - v_1(\xi,\tau) = 0,\\ \partial_\tau v_1(\xi,\tau) + \partial_\xi v_2(\xi,\tau) + u_1(\xi,\tau) = 0,\\ -\partial_\tau u_2(\xi,\tau) - \partial_\xi u_1(\xi,\tau) - v_2(\xi,\tau) = 0,\\ -\partial_\tau v_2(\xi,\tau) - \partial_\xi v_1(\xi,\tau) + u_2(\xi,\tau) = 0,\\ u_1(\xi,0) = \xi^2 - \xi + 1/6,\\ v_1(\xi,0) = 0,\\ u_2(\xi,0) = \begin{cases}\xi - 0.25, & 0 \le \xi \le 1/2\\ -\xi + 0.75, & 1/2 \le \xi \le 1\end{cases}\\ v_2(\xi,0) = 0,\\ u_1(0,\tau) = u_1(1,\tau),\\ v_1(0,\tau) = v_1(1,\tau),\\ u_2(0,\tau) = u_2(1,\tau),\\ v_2(0,\tau) = v_2(1,\tau).\end{cases} \tag{24}$$

Assuming that $C_n^2 = 0, C_n^4 = 0$ corresponding approximated solution is

$$u_1(\xi,\tau) = \sum_{n=1}^{80}\Bigg(C_n^1\begin{pmatrix}1\\ -\alpha_n\end{pmatrix}\Big(\cos(2\pi n\xi)\cos(\sqrt{4\pi^2n^2+1}\tau) + \sin(2\pi n\xi)\sin(\sqrt{4\pi^2n^2+1}\tau)\Big)$$

$$+C_n^3\begin{pmatrix}1\\ \alpha_n^{-1}\end{pmatrix}\Big(\cos(2\pi n\xi)\cos(\sqrt{4\pi^2n^2+1}\tau) + \sin(2\pi n\xi)\sin(\sqrt{4\pi^2n^2+1}\tau)\Big)$$

$$u_2(\xi,\tau) = \sum_{n=1}^{80}\Bigg(D_n^1\begin{pmatrix}1\\ -\alpha_n\end{pmatrix}\Big(\cos(2\pi n\xi)\cos(\sqrt{4\pi^2n^2+1}\tau) + \sin(2\pi n\xi)\sin(\sqrt{4\pi^2n^2+1}\tau)\Big)$$

$$+D_n^3\begin{pmatrix}1\\ -\alpha_n^{-1}\end{pmatrix}\Big(\cos(2\pi n\xi)\cos(\sqrt{4\pi^2n^2+1}\tau) + \sin(2\pi n\xi)\sin(\sqrt{4\pi^2n^2+1}\tau)\Big)$$

$$v_1(\xi,\tau) = 0, \quad v_2(\xi,\tau) = 0$$

Below are illustrated graphs of solutions $u_1(\xi,\tau)$ and $u_2(\xi,\tau)$ for any $\xi \in [0,1]$ and $\tau_1 = 0.0$, $\tau_2 = \pi/4 \sim 0.79$ and $\tau_3 = \pi/2 \sim 1.57$.

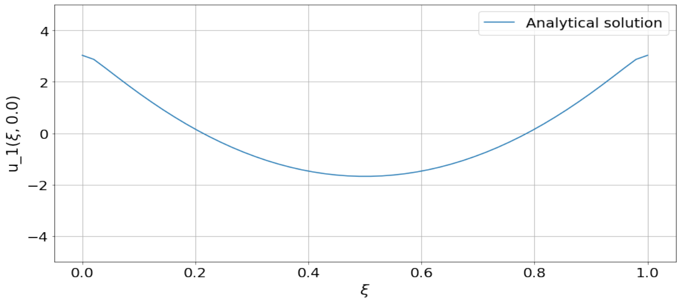

FIGURE 23. Graph of $u_1(\xi, 0)$

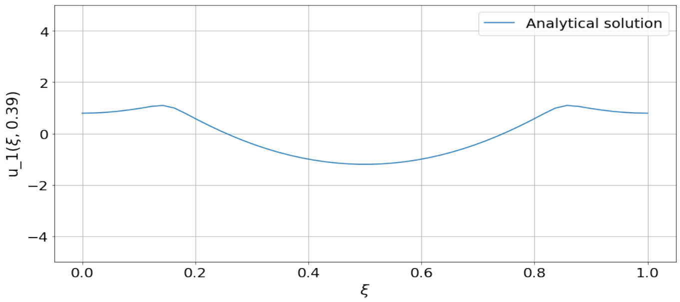

FIGURE 24. Graph of $u_1(\xi, 0.39)$

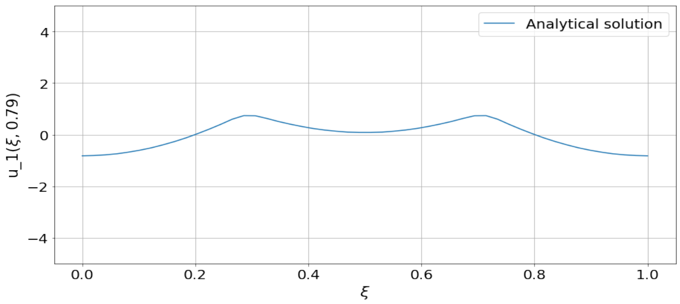

FIGURE 25. Graph of $u_1(\xi, 0.79)$

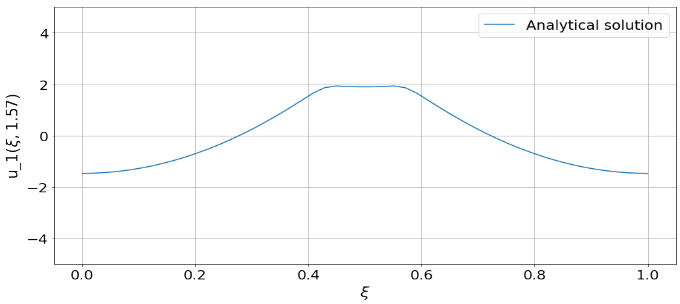

FIGURE 26. Graph of $u_1(\xi, 1.57)$

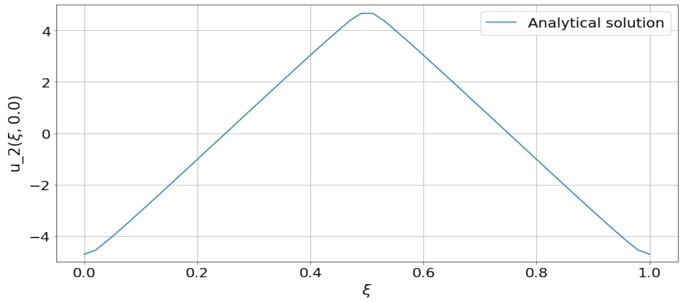

FIGURE 27. Graph of $u_2(\xi, 0)$

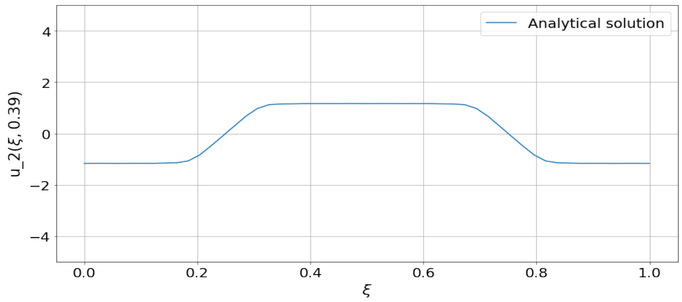

FIGURE 28. Graph of $u_2(\xi, 0.39)$

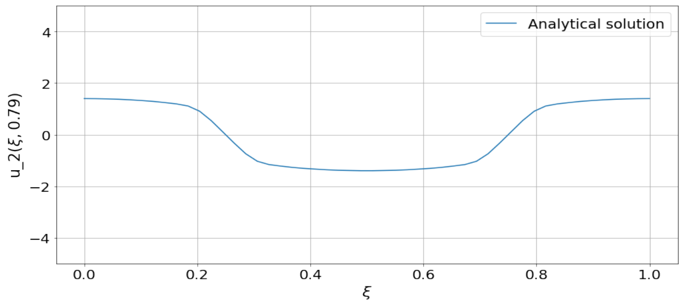

FIGURE 29. Graph of $u_2(\xi, 0.79)$

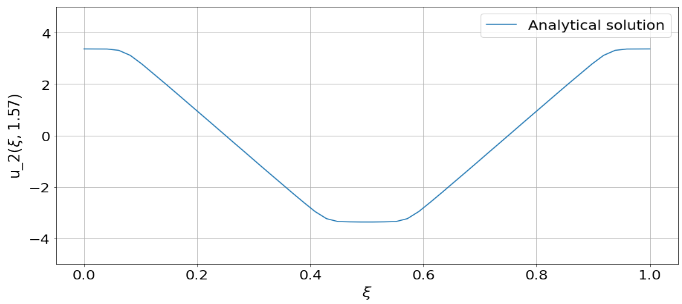

FIGURE 30. Graph of $u_2(\xi, 1.57)$

3. Nonlinear Dirac Equation in (1+1) dimension

In this section we consider Nonlinear Dirac equation in (1+1) dimension with cubic term (see for example [13])

$$i(\partial_\tau + \alpha\partial_\xi)\psi + \beta\psi = <\beta\psi, \psi> \beta\psi, \tag{25}$$

where,

$$\alpha = \begin{pmatrix} 0 & 1 \\ 1 & 0 \end{pmatrix}, \quad \text{and} \quad \beta = \begin{pmatrix} 1 & 0 \\ 0 & -1 \end{pmatrix},$$

are hermitian (2×2) matrices satisfying $\beta^2 = \alpha^2 = \mathbb{I}$ and anticommutation relation $\alpha\beta + \beta\alpha = 0$, and $<,>$ is a C^2- scalar product.

Thus, Nonlinear Dirac equation in (1+1) dimension is:

$$\begin{cases} i\partial_\tau\psi_1(\xi,\tau) + i\partial_\xi\psi_2(\xi,\tau) + \psi_1(\xi,\tau) & = \psi_1(\xi,\tau)\left(|\psi_1(\xi,\tau)|^2 - |\psi_2(\xi,\tau)|^2\right), \\ i\partial_\tau\psi_2(\xi,\tau) + i\partial_\xi\psi_1(\xi,\tau) - \psi_2(\xi,\tau) & = -\psi_2(\xi,\tau)\left(|\psi_1(\xi,\tau)|^2 - |\psi_2(\xi,\tau)|^2\right) \end{cases} \tag{26}$$

Our aim here is to examine plane wave solutions of Nonlinear Dirac equation in (1+1) dimension and provide an example of initial boundary value problem.

3.1. **Plane wave solutions.**

Lemma 3.1. *The Nonlinear Dirac equation in (1+1) dimension*

$$\begin{cases} i\partial_\tau\psi_1(\xi,\tau) + i\partial_\xi\psi_2(\xi,\tau) + \psi_1(\xi,\tau) & = \psi_1(\xi,\tau)\left(|\psi_1(\xi,\tau)|^2 - |\psi_2(\xi,\tau)|^2\right), \\ i\partial_\tau\psi_2(\xi,\tau) + i\partial_\xi\psi_1(\xi,\tau) - \psi_2(\xi,\tau) & = -\psi_2(\xi,\tau)\left(|\psi_1(\xi,\tau)|^2 - |\psi_2(\xi,\tau)|^2\right) \end{cases} \tag{27}$$

admits plane wave solutions of type

$$\psi_j(\xi,\tau) = a_j \exp\left[i(k\xi - \omega\tau)\right], j = 1, 2,$$

provided that

$$k = \frac{2a_1a_2\left(1 - a_1^2 + a_2^2\right)}{a_2^2 - a_1^2}, \quad \omega = \frac{\left(a_1^2 + a_2^2\right)\left(1 - a_1^2 + a_2^2\right)}{a_2^2 - a_1^2},$$

where $a_2^2 - a_1^2 \neq 0$.

Proof. First let's rewrite solution conveniently

$$\begin{cases} \psi_1(\xi,\tau) = a_1 e^{i(k\xi - \omega\tau)}, \\ \psi_2(\xi,\tau) = a_2 e^{i(k\xi - \omega\tau)}. \end{cases}$$

and find partial derivatives

$$\partial_\tau\psi(\xi,\tau) = \begin{cases} -i\omega a_1 e^{i(k\xi-\omega\tau)}, \\ -i\omega a_2 e^{i(k\xi-\omega\tau)} \end{cases}, \quad \partial_\xi\psi(\xi,\tau) = \begin{cases} ika_1 e^{i(k\xi-\omega\tau)}, \\ ika_2 e^{i(k\xi-\omega\tau)}. \end{cases}$$

Plug in (27):

$$\begin{bmatrix} \omega a_1 e^{i(k\xi-\omega\tau)} \\ \omega a_2 e^{i(k\xi-\omega\tau)} \end{bmatrix} - \begin{bmatrix} ka_2 e^{i(k\xi-\omega\tau)} \\ ka_1 e^{i(k\xi-\omega\tau)} \end{bmatrix} + \begin{bmatrix} a_1 e^{i(k\xi-\omega\tau)} \\ -a_2 e^{i(k\xi-\omega\tau)} \end{bmatrix}$$
$$= \begin{bmatrix} a_1 e^{i(k\xi-\omega\tau)}\left(a_1^2 e^{2i(k\xi-\omega\tau)} - a_2^2 e^{2i(k\xi-\omega\tau)}\right) \\ -a_2 e^{i(k\xi-\omega\tau)}\left(a_1^2 e^{2i(k\xi-\omega\tau)} - a_2^2 e^{2i(k\xi-\omega\tau)}\right) \end{bmatrix}$$

Which can be rewritten as follows:

$$\begin{bmatrix} \omega a_1 \\ \omega a_2 \end{bmatrix} - \begin{bmatrix} ka_2 \\ ka_1 \end{bmatrix} + \begin{bmatrix} a_1 \\ -a_2 \end{bmatrix} = \begin{bmatrix} a_1\left(a_1^2 - a_2^2\right) \\ -a_2\left(a_1^2 - a_2^2\right) \end{bmatrix}$$

We can rewrite it as a system

$$\begin{cases} \omega a_1 - k a_2 + a_1 = a_1 \left(a_1^2 - a_2^2\right), \\ \omega a_2 - k a_1 - a_2 = -a_2 \left(a_1^2 - a_2^2\right) \end{cases} \tag{28}$$

Multiply first part of the system to (28) a_2 and second part to a_1 :

$$\begin{cases} \omega a_1 a_2 - k a_2^2 + a_1 a_2 = a_1 a_2 \left(a_1^2 - a_2^2\right), \\ \omega a_2 a_1 - k a_1^2 - a_2 a_1 = -a_2 a_1 \left(a_1^2 - a_2^2\right) \end{cases}$$

Sum them up and subtract:

$$\begin{cases} 2\omega a_1 a_2 - k a_2^2 - k a_1^2 a_1 a_2 = 0, \\ -k a_2^2 - k a_1^2 + 2 a_2 a_1 = 2 a_2 a_1 \left(a_1^2 - a_2^2\right) \end{cases}$$

Solving the above system leads to:

$$k = \frac{2 a_1 a_2 \left(1 - a_1^2 + a_2^2\right)}{a_2^2 - a_1^2}, \quad \omega = \frac{\left(a_1^2 + a_2^2\right)\left(1 - a_1^2 + a_2^2\right)}{a_2^2 - a_1^2}$$

□

3.1.1. *Example 3.* In this subsection we consider an example of initial boundary value problem for Nonlinear Dirac equation in (1+1) dimension.

Example 3. *The Nonlinear Dirac equation in (1+1) dimension for any* $\xi \in [0,1]$ *and* $\tau \in [0, \pi/2]$:

$$\begin{cases} i\partial_\tau \psi_1(\xi,\tau) + i\partial_\xi \psi_2(\xi,\tau) + \psi_1(\xi,\tau) & = \psi_1(\xi,\tau)\left(|\psi_1(\xi,\tau)|^2 - |\psi_2(\xi,\tau)|^2\right), \\ i\partial_\tau \psi_2(\xi,\tau) + i\partial_\xi \psi_1(\xi,\tau) - \psi_2(\xi,\tau) & = -\psi_2(\xi,\tau)\left(|\psi_1(\xi,\tau)|^2 - |\psi_2(\xi,\tau)|^2\right), \\ \psi_1(0,\tau) = \psi_1(1,\tau), \\ \psi_2(0,\tau) = \psi_2(1,\tau), \\ \psi_1(\xi,0) = 2.827 e^{2i\pi\xi}, \\ \psi_2(\xi,0) = e^{2i\pi\xi}. \end{cases}$$

has the plane wave solution:

$$\begin{cases} \psi_1(\xi,\tau) = 2.827 e^{i(2\pi\xi - 3.413\tau)}, \\ \psi_2(\xi,\tau) = e^{i(2\pi\xi - 3.413\tau)}. \end{cases}$$

This solution can be obtained by Lemma 3.1 with specific parameters

$$k = 2\pi, \quad \omega = 3.413, \quad a_1 = 2.827 \quad \text{and} \quad a_2 = 1.$$

Since our PDE is complex, we can separate it to real and imaginary parts:

$$\begin{cases} \psi_1(\xi,\tau) = u_1(\xi,\tau) + i v_1(\xi,\tau), \\ \psi_2(\xi,\tau) = u_2(\xi,\tau) + i v_2(\xi,\tau) \end{cases}$$

which leads to

$$
\begin{cases}
\partial_\tau v_1 - \partial_\xi v_2 + u_1 - u_1^3 - u_1 v_1^2 + u_1 u_2^2 + u_1 v_1^2 = 0,\\
\partial_\tau u_1 + \partial_\xi u_2 + v_1 - v_1 u_1^2 - v_1^3 + v_1 u_2^2 - v_1 v_2^2 = 0,\\
-\partial_\tau v_2 - \partial_\xi v_1 - u_2 + u_2 u_1^2 + u_2 v_1^2 - u_2^3 - u_2 v_2^2 = 0,\\
-\partial_\tau u_2 + \partial_\xi u_1 - v_2^2 + v_2 u_1^2 + v_2 v_1^2 - v_2^3 - v_2 u_2^2 = 0,\\
u_1(\xi,0) = 2.827\cos 2\pi\xi,\\
v_1(\xi,0) = 2.827\sin 2\pi\xi,\\
u_2(\xi,0) = \cos 2\pi\xi,\\
v_2(\xi,0) = \sin 2\pi\xi,\\
u_1(0,\tau) = u_1(1,\tau),\\
v_1(0,\tau) = v_1(1,\tau),\\
u_2(0,\tau) = u_2(1,\tau),\\
v_2(0,\tau) = v_2(1,\tau).
\end{cases} \tag{29}
$$

Its corresponding solution is

$$
\begin{cases}
u_1(\xi,\tau) = 2.827\cos(2\pi\xi - 3.413\tau),\\
v_1(\xi,\tau) = 2.827\sin(2\pi\xi - 3.413\tau),\\
u_2(\xi,\tau) = \cos(2\pi\xi - 3.413\tau),\\
v_2(\xi,\tau) = \sin(2\pi\xi - 3.413\tau),
\end{cases}
$$

Below are illustrated graphs of $u_1(\xi,\tau), v_1(\xi,\tau), u_2(\xi,\tau)$ and $v_2(\xi,\tau)$ for any $\xi \in [0,1]$ and $\tau_1 = 0, \tau_2 = \pi/4 \sim 0.79$ and $\tau_3 = \pi/2 \sim 1.57$.

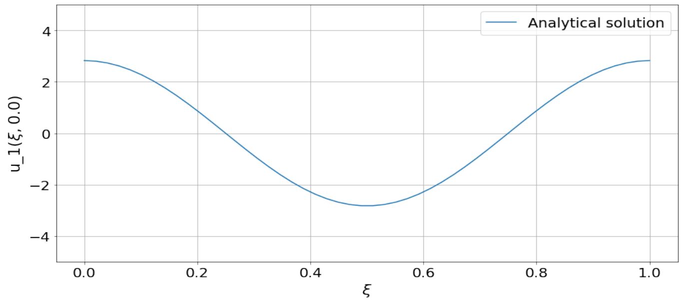

FIGURE 31. Graph of $u_1(\xi, 0)$

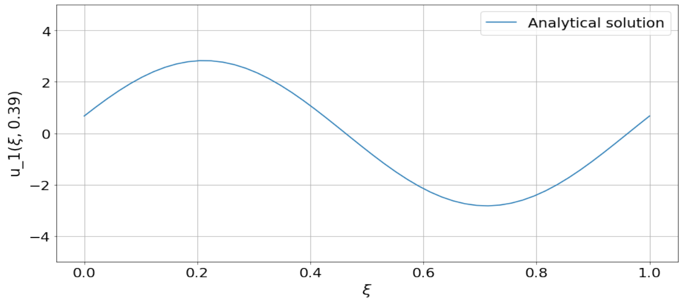

FIGURE 32. Graph of $u_1(\xi, 0.39)$

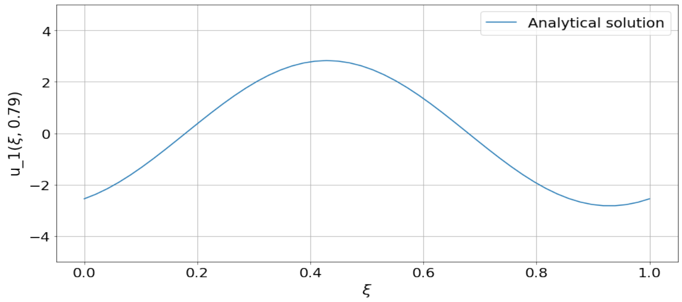

FIGURE 33. Graph of $u_1(\xi, 0.79)$

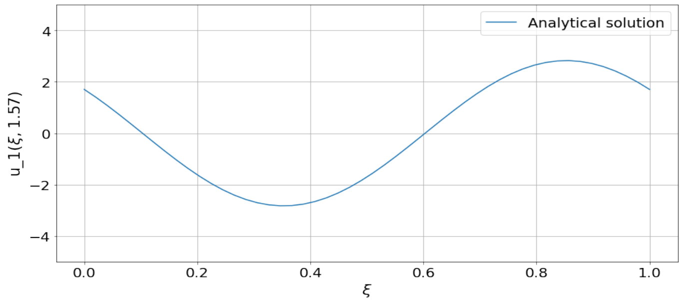

FIGURE 34. Graph of $u_1(\xi, 1.57)$

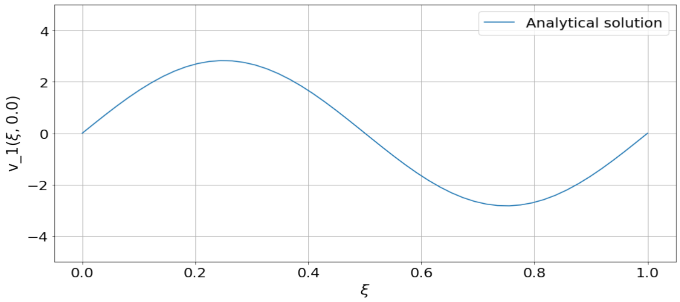

FIGURE 35. Graph of $v_1\,(\xi, 0)$

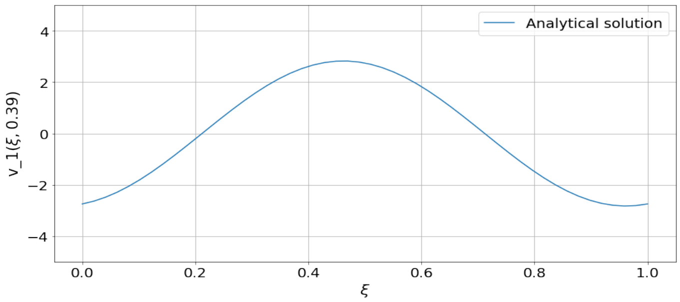

FIGURE 36. Graph of $v_1\,(\xi, 0.39)$

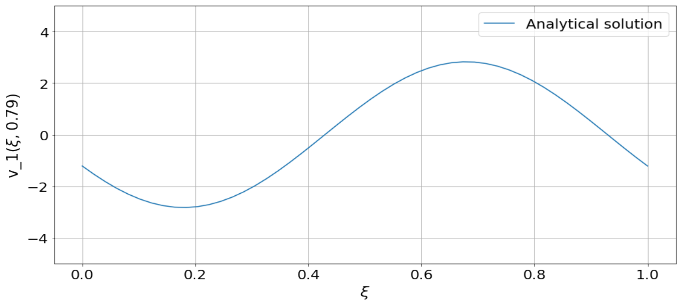

FIGURE 37. Graph of $v_1\,(\xi, 0.79)$

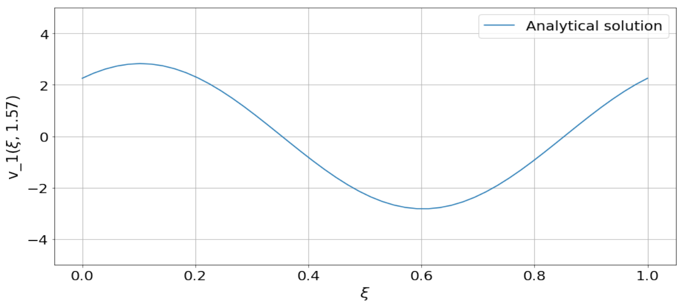

FIGURE 38. Graph of $v_1\,(\xi, 1.57)$

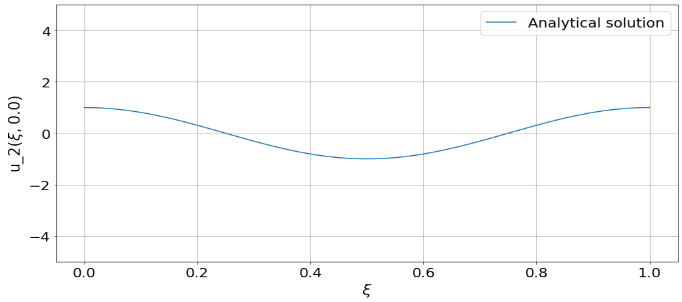

FIGURE 39. Graph of $u_2\,(\xi, 0)$

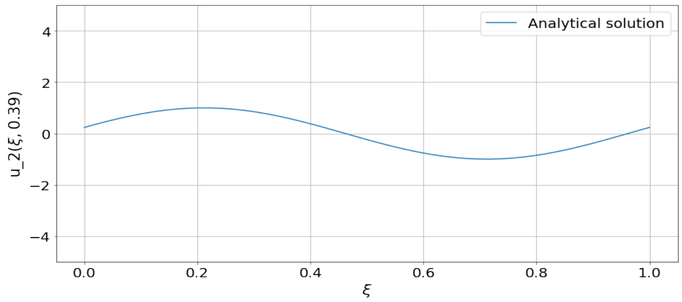

FIGURE 40. Graph of $u_2\,(\xi, 0.39)$

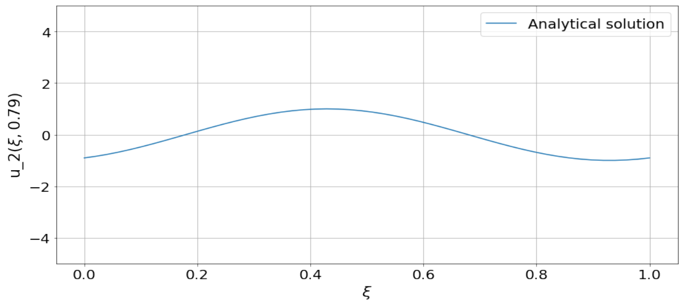

FIGURE 41. Graph of $u_2\,(\xi, 0.79)$

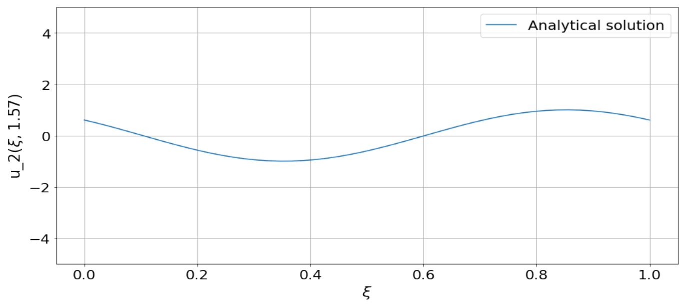

FIGURE 42. Graph of $u_2\,(\xi, 1.57)$

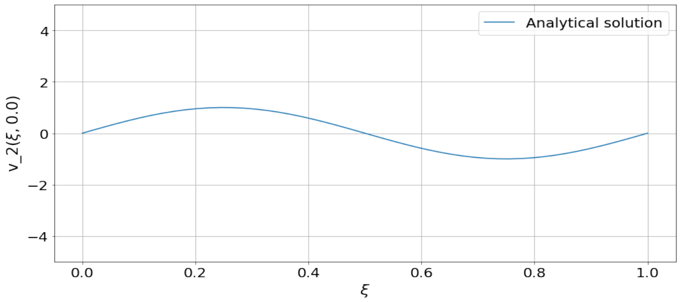

FIGURE 43. Graph of $v_2\,(\xi, 0)$

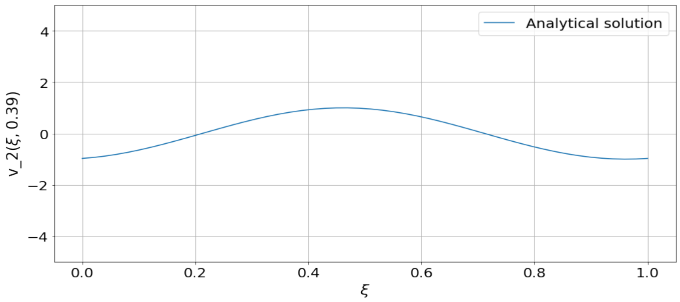

FIGURE 44. Graph of $v_2\,(\xi, 0.39)$

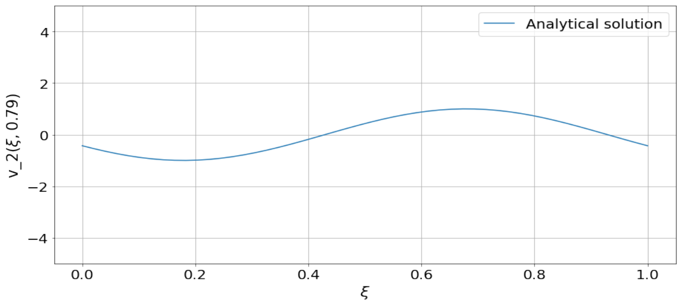

FIGURE 45. Graph of $v_2\,(\xi, 0.79)$

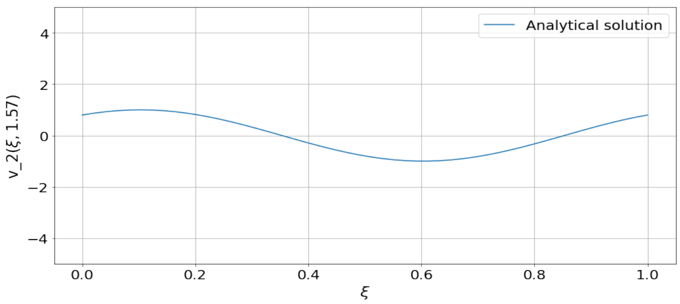

FIGURE 46. Graph of $v_2\,(\xi, 1.57)$

4. Machine learning for Dirac equation

4.1. **Neural Networks.** These days artificial neural networks are entering most spheres of science and technology and major role of working with neural networks is the modeling where the main emphasis is on learning the model and tuning the hyperparameters. Indeed, neural networks is a composition of nonlinear operations where each of them imposed by parameters which have to be evaluated from given data. Therefore the results of predicted values might vary according to the architecture and learning parameters which have been used. There can be a number of hidden layers, learning rate, weight and biases,etc. Consequently, hyperparameter tuning is the most important part of training the model.

In our study we consider feedforward neural networks which is the classical category of deep neural networks. In the following picture we can see that architecture of multilayer feedforward neural networks consists of n inputs, n hidden layers and n output layers.

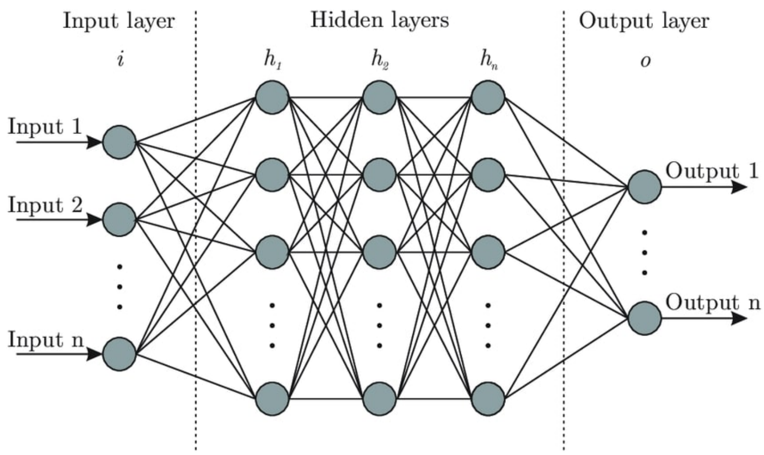

FIGURE 47. Feedforward Neural Networks

Feedforward neural networks are defined as follows:

$$h^l(x) = W^l\sigma\left(h^{l-1}(x)\right) + b^l \in \mathbb{R}^{N_l}, \quad \text{for} \quad 2 \le l \le L,$$

where each layer can have its own input and output dimensions, the only requirement is that the input dimension for layer l is the output dimension of layer $l-1$ and we learn it to satisfy initial, boundary conditions and adjust hyperparameters to minimize loss function.

4.2. **Physics Informed Neural Networks.** Purpose of this section is to create an architecture of multilayer feedforward neural networks to obtain approximate solutions of Dirac equation in (1+1) dimension and we follow the idea of Physics Informed Neural Networks (PINNs). Programming language that we use is Python and codes can be found in the following link:PINNs for Dirac equation in (1+1) dimension. Consider following steps which are essential in creating a code.

Step 1: First of all, we import libraries, which we are going to work. They are *keras*, *tensorflow*, *numpy*, and *matplotlib*. *Keras* is a network library, *Tensorflow* is an open source library for machine learning tasks, *numpy* will be used to save our values and *matplotlib* to plot our graphs of solutions.

Step 2: Every machine learning procedure starts with data collection and in our case data is taken from randomly sampled points from space $\xi \in [0,1]$ and time $\tau \in [0,\pi/2]$. For initial value and boundary condition points we took $N_{IC} = N_{BC} = 1000$. As for collocation points we decided to take $N_{CF} = 20000$ and we have experimented with 500 epochs. In machine learning community term epoch is to used to indicate number of passes in the training data that an algorithm completed.

Below are illustrated pictures of initial, boundary and collocation points.

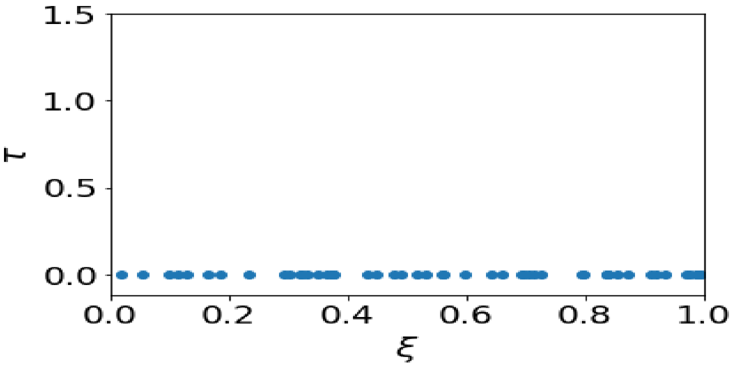

FIGURE 48. Initial condition points

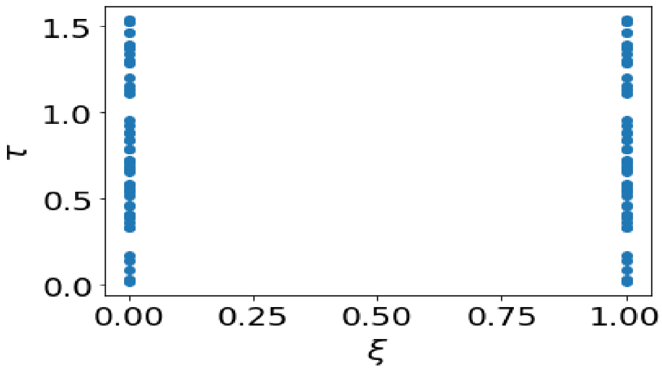

FIGURE 49. Boundary condition points

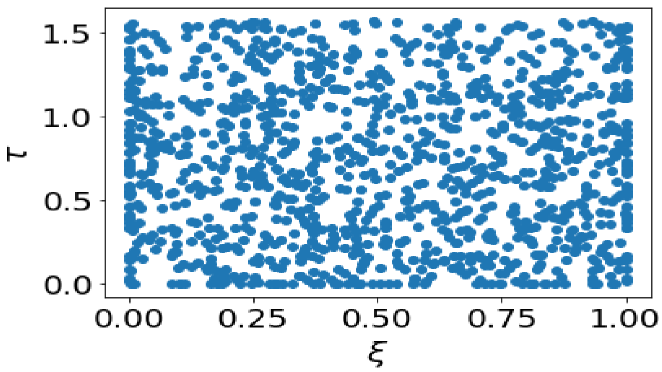

FIGURE 50. Collocation points

Step 3: Introduce initial conditions which are separated to real and imaginary parts: $u_1(\xi,0), v_1(\xi,0), u_2(\xi,0)$ and $v_2(\xi,0)$.

Step 4: Introduce periodic boundary conditions which are separated to real and imaginary parts: $u_1(0,\tau) = u_1(1,\tau), v_1(0,\tau) = v_1(1,\tau)$, $u_2(0,\tau) = u_2(1,\tau), v_2(0,\tau) = v_2(1,\tau)$.

Step 5: Create input data according to initial, boundary conditions and collocation points.

Step 6: Introduce activation functions. Main role of activation functions is adding nonlinearity which prevents an issue of vanishing gradient, which completely stops the neural network for further learning. Popular choices of activation functions are :

- sigmoid $\varphi(x) = \frac{1}{1+e^{-x}}$
- hyperbolic tangent $\varphi(x) = tanhx$
- rectified linear unit $\varphi(x) = \max\{x,0\}$

and in our study we decide to use hyperbolic tangent activation function referring to [14].

Step 7: Output data consists on four predicted solutions $\tilde{u}_1, \tilde{v}_1, \tilde{u}_2$ and $\tilde{v}_2$ which we need to find.

Step - 8: To measure an accuracy of our network in our experiments we use Mean Squared Error Loss function:

$$\begin{aligned} MSE &= \omega_1 MSE_1 + \omega_2 MSE_2 + \omega_3 MSE_3 + \omega_4 MSE_4 \\ &+ \omega_5 MSE_5 + \omega_6 MSE_6 + \omega_7 MSE_7 + \omega_8 MSE_8 \\ &+ \omega_9 MSE_9 + \omega_{10} MSE_{10} + \omega_{11} MSE_{11} + \omega_{12} MSE_{12}, \end{aligned}$$

where $\omega_1, \dots, \omega_{12}$ are weights of each loss function to fix conveniently later;

$$MSE_1 = \frac{1}{N_{IC}} \sum_{i=1}^{N_{IC}} |u_1(\xi^i_{IC}, 0) - \tilde{u}_1(\xi^i_{IC}, 0)|^2, \quad MSE_2 = \frac{1}{N_{IC}} \sum_{i=1}^{N_{IC}} |v_1(\xi^i_{IC}, 0) - \tilde{v}_1(\xi^i_{IC}, 0)|^2$$

$$MSE_3 = \frac{1}{N_{IC}} \sum_{i=1}^{N_{IC}} |u_2(\xi^i_{IC}, 0) - \tilde{u}_2(\xi^i_{IC}, 0)|^2, \quad MSE_4 = \frac{1}{N_{IC}} \sum_{i=1}^{N_{IC}} |v_2(\xi^i_{IC}, 0) - \tilde{v}_2(\xi^i_{IC}, 0)|^2$$

$$MSE_5 = \frac{1}{N_{BC}} \sum_{i=1}^{N_{BC}} |\tilde{u}_1(0, \tau^i_{BC}) - \tilde{u}_1(1, \tau^i_{BC})|^2, \quad MSE_6 = \frac{1}{N_{BC}} \sum_{i=1}^{N_{BC}} |\tilde{v}_1(0, \tau^i_{BC}) - \tilde{v}_1(0, \tau^i_{BC})|^2$$

$$MSE_7 = \frac{1}{N_{BC}} \sum_{i=1}^{N_{BC}} |\tilde{u}_2(0, \tau^i_{BC}) - \tilde{u}_2(1, \tau^i_{BC})|^2, \quad MSE_8 = \frac{1}{N_{BC}} \sum_{i=1}^{N_{BC}} |\tilde{v}_2(0, \tau^i_{BC}) - \tilde{v}_2(1, \tau^i_{BC})|^2$$

$$MSE_9 = \frac{1}{N_{CF}} \sum_{i=1}^{N_{CF}} |f_1(\tilde{u}_1(\xi^i_{CF}, \tau^i_{CF}), \tilde{v}_1(\xi^i_{CF}, \tau^i_{CF}), \tilde{u}_2(\xi^i_{CF}, \tau^i_{CF}), \tilde{v}_2(\xi^i_{CF}, \tau^i_{CF}))|^2,$$

$$MSE_{10} = \frac{1}{N_{CF}} \sum_{i=1}^{N_{CF}} |f_2(\tilde{u}_1(\xi^i_{CF}, \tau^i_{CF}), \tilde{v}_1(\xi^i_{CF}, \tau^i_{CF}), \tilde{u}_2(\xi^i_{CF}, \tau^i_{CF}), \tilde{v}_2(\xi^i_{CF}, \tau^i_{CF}))|^2,$$

$$MSE_{11} = \frac{1}{N_{CF}} \sum_{i=1}^{N_{CF}} |f_3(\tilde{u}_1(\xi^i_{CF}, \tau^i_{CF}), \tilde{v}_1(\xi^i_{CF}, \tau^i_{CF}), \tilde{u}_2(\xi^i_{CF}, \tau^i_{CF}), \tilde{v}_2(\xi^i_{CF}, \tau^i_{CF}))|^2,$$

$$MSE_{12} = \frac{1}{N_{CF}} \sum_{i=1}^{N_{CF}} |f_4(\tilde{u}_1(\xi^i_{CF}, \tau^i_{CF}), \tilde{v}_1(\xi^i_{CF}, \tau^i_{CF}), \tilde{u}_2(\xi^i_{CF}, \tau^i_{CF}), \tilde{v}_2(\xi^i_{CF}, \tau^i_{CF}))|^2,$$

Let's consider each block of MSE in detail: $MSE_1, \ldots, MSE_4-$ are MSEs corresponding to initial conditions, $MSE_5, \ldots, MSE_8-$ for boundary conditions and $MSE_9, \ldots, MSE_{12}$ for PDE itself.

As for $f_1(u), f_1(v), f_1(v)$ and $f_2(v)$, they are defined as follows:

$$\tilde{u}_1, \tilde{v}_1, \tilde{u}_2, \tilde{v}_2 = \tilde{u}_1(\xi^i_{CF}, \tau^i_{CF}), \tilde{v}_1(\xi^i_{CF}, \tau^i_{CF}), \tilde{u}_2(\xi^i_{CF}, \tau^i_{CF}), \tilde{v}_2(\xi^i_{CF}, \tau^i_{CF})$$

for experiments (1) and (2)

$$f_1(\tilde{u}_1, \tilde{v}_1, \tilde{u}_2, \tilde{v}_2) = \partial_\tau u_1 (\xi, \tau) + \partial_\xi u_2 (\xi, \tau) - v_1 (\xi, \tau),$$

$$f_2(\tilde{u}_1, \tilde{v}_1, \tilde{u}_2, \tilde{v}_2) = \partial_\tau v_1 (\xi, \tau) + \partial_\xi v_2 (\xi, \tau) + u_1 (\xi, \tau),$$

$$f_3(\tilde{u}_1, \tilde{v}_1, \tilde{u}_2, \tilde{v}_2) = -\partial_\tau u_2 (\xi, \tau) - \partial_\xi u_1 (\xi, \tau) - v_2 (\xi, \tau),$$

$$f_4(\tilde{u}_1, \tilde{v}_1, \tilde{u}_2, \tilde{v}_2) = -\partial_\tau v_2 (\xi, \tau) - \partial_\xi v_1 (\xi, \tau) + u_2 (\xi, \tau).$$

and for experiment (3.1.1)

$$f_1(\tilde{u}_1, \tilde{v}_1, \tilde{u}_2, \tilde{v}_2) = \partial_\tau v_1 - \partial_\xi v_2 + u_1 - u_1^3 - u_1 v_1^2 + u_1 u_2^2 + u_1 v_1^2,$$

$$f_2(\tilde{u}_1, \tilde{v}_1, \tilde{u}_2, \tilde{v}_2) = \partial_\tau u_1 + \partial_\xi u_2 + v_1 - v_1 u_1^2 - v_1^3 + v_1 u_2^2 - v_1 v_2^2,$$

$$f_3(\tilde{u}_1, \tilde{v}_1, \tilde{u}_2, \tilde{v}_2) = -\partial_\tau v_2 - \partial_\xi v_1 - u_2 + u_2 u_1^2 + u_2 v_1^2 - u_2^3 - u_2 v_2^2,$$

$$f_4(\tilde{u}_1, \tilde{v}_1, \tilde{u}_2, \tilde{v}_2) = \partial_\tau u_2 + \partial_\xi u_1 - v_2 + v_2 u_1^2 + v_2 v_1^2 - v_2^3 - v_2 u_2^2$$

Therefore, the main of idea of PINNs is to provide an approximate solution of PDE taking input data from initial and boundary condition, setting PDE which plays the role of regularizer and produce predicted solutions.

Below is illustrated schematic picture of PINNs for Linear Dirac equation in (1+1) dimension:

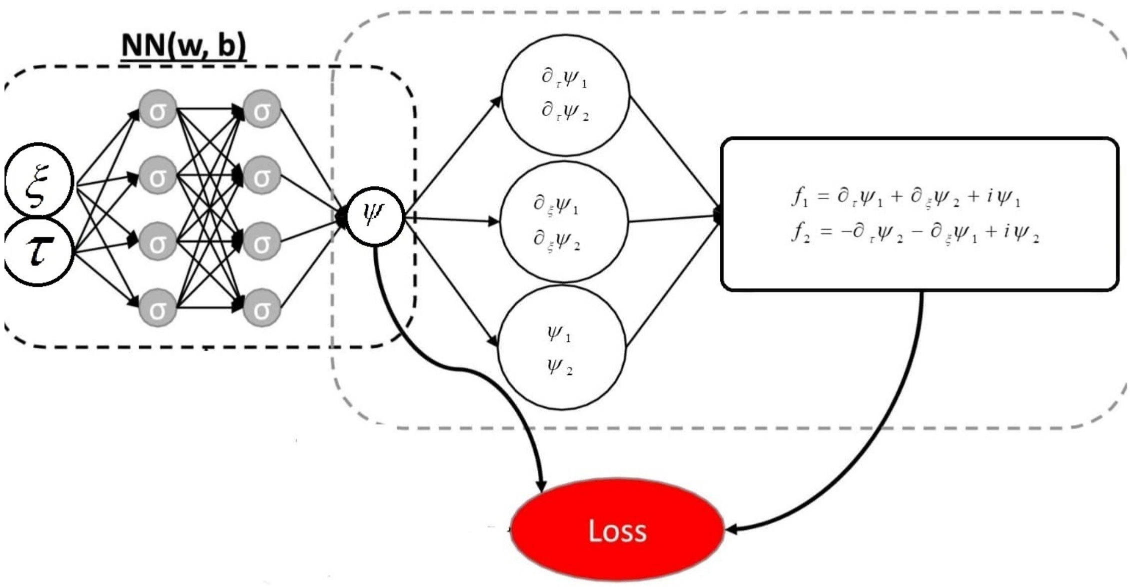

FIGURE 51. Schematic picture of PINNs for Linear Dirac equation in (1+1) dimension

4.3. **Experiments.** The aim of this section is to approximate the solution of the Linear and Nonlinear Dirac equation in (1+1) dimension from a set of training data and solve it applying multilayer feedforward Physics Informed Neural Networks.

In our experiments we follow the idea of [14] and started by choosing all weights to be $\omega_1, \dots, \omega_{12} = 1$. However, our obtained solutions were poor. Moreover, [18] also noted that taking equal weights for each loss does not always provide optimal solutions for PDEs and proposed an algorithm for single hidden layer. Nevertheless, we observed that taking 1 or 2 layers does not show good results.

Layers	Neurons	MSE u_1	MSE v_1	MSE u_2	MSE v_2
2	10	0.1530	0.1581	0.9977	0.1795
4	20	0.1762	0.2214	0.2084	0.2403
6	20	0.1716	0.1895	0.1947	0.2151
8	10	0.1929	0.1631	0.2143	0.1899
9	20	0.0140	0.0022	0.0148	0.0026

TABLE 1. Comparison table of layers for $N_{IC} = 1000, N_{BC} = 1000, N_{CF} = 20000$, epochs = 500

Hence, in our experiments we decided to choose different weights implemented to the examples discussed in previous sections:

- Example 1
- Example 2
- Example 3.1.1

4.3.1. *Experiment 1.* The purpose of this experiment is to test PINNs for the Example 1 in the following cases:

- with emphasis on Initial Value Loss,
- with emphasis on Boundary Condition Value Loss,
- with emphasis on PDE Loss.

For each of them we test at times:

- $\tau = 0$,
- $\tau = \pi/8 \sim 0.39$,
- $\tau = \pi/4 \sim 0.79$,
- $\tau = \pi/2 \sim 1.57$.

Let's start with experiment on emphasis of Initial Value Loss, which is the case when $\omega_1 = \dots = \omega_4 = 100$ and $\omega_5 = \dots = \omega_{12} = 1$.

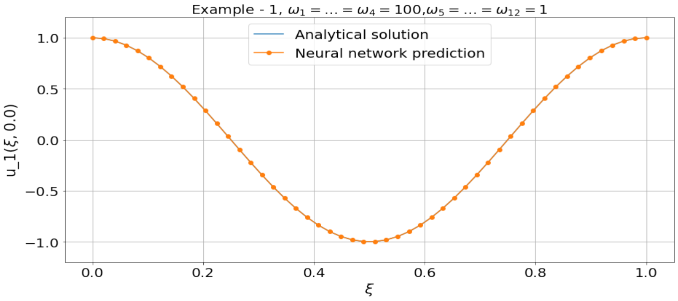

FIGURE 52. Graph of $u_1(\xi, 0)$

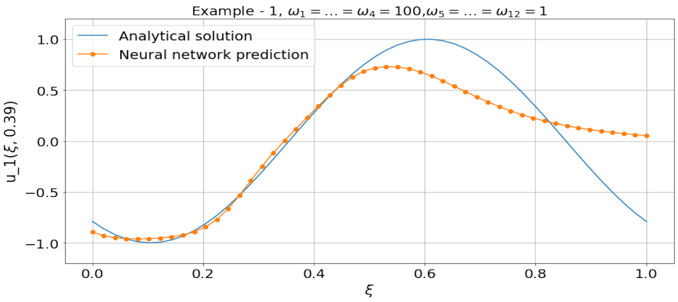

FIGURE 53. Graph of $u_1(\xi, 0.39)$

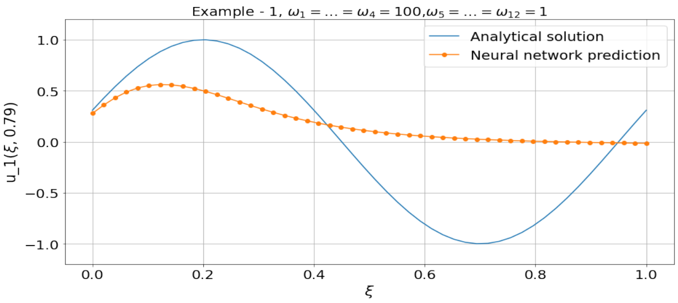

FIGURE 54. Graph of $u_1(\xi, 0.79)$

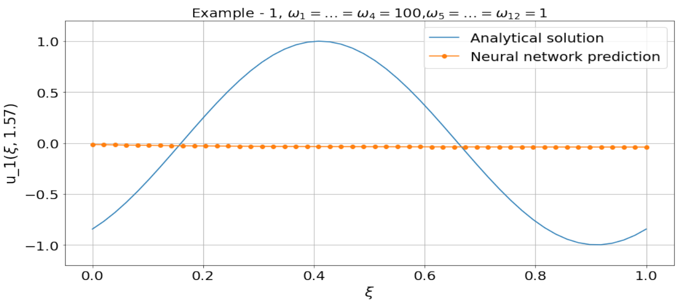

FIGURE 55. Graph of $u_1(\xi, 1.57)$

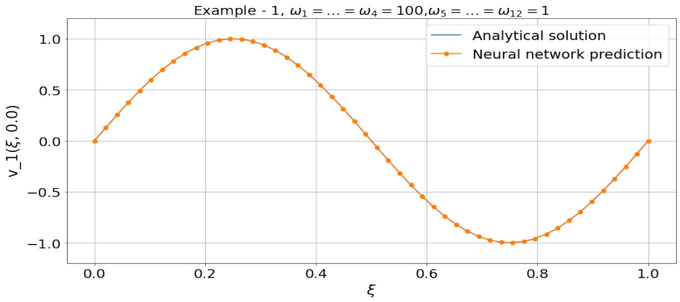

FIGURE 56. Graph of $v_1(\xi, 0)$

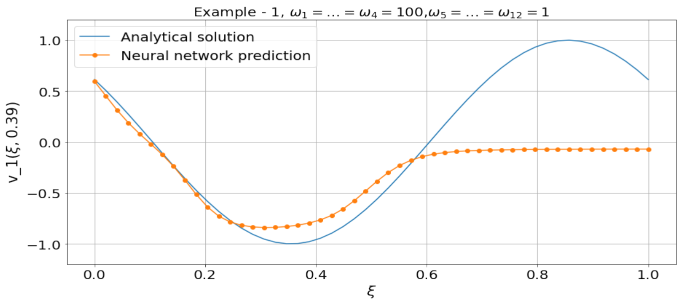

FIGURE 57. Graph of $v_1(\xi, 0.39)$

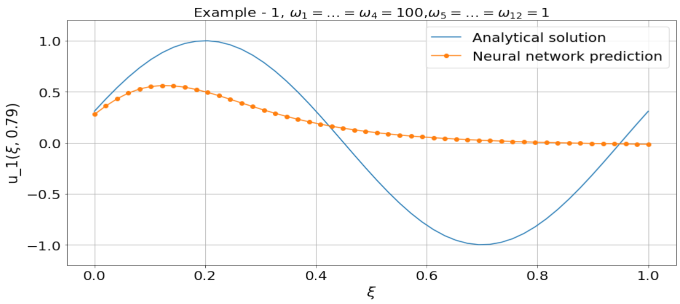

FIGURE 58. Graph of $v_1(\xi, 0.79)$

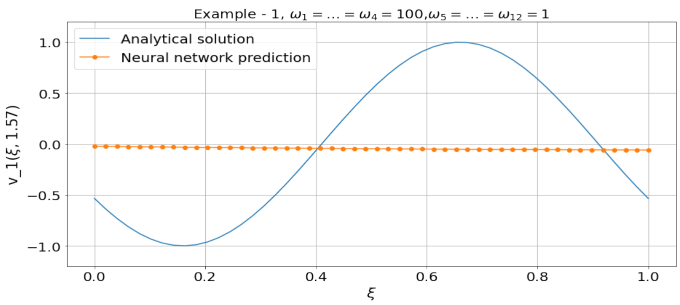

FIGURE 59. Graph of $v_1(\xi, 1.57)$

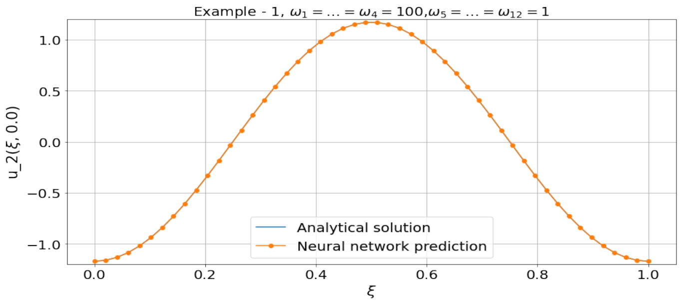

FIGURE 60. Graph of $u_2(\xi, 0)$

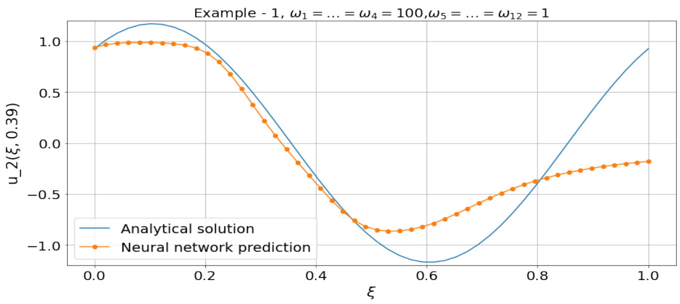

FIGURE 61. Graph of $u_2(\xi, 0.39)$

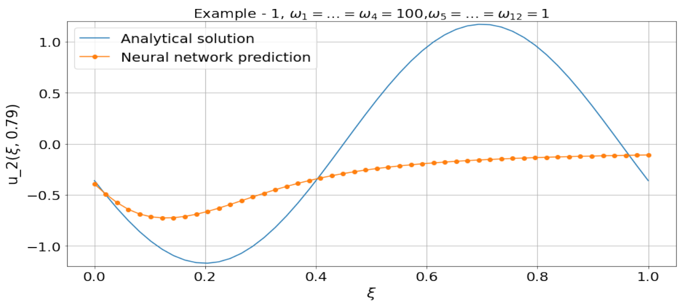

FIGURE 62. Graph of $u_2(\xi, 0.79)$

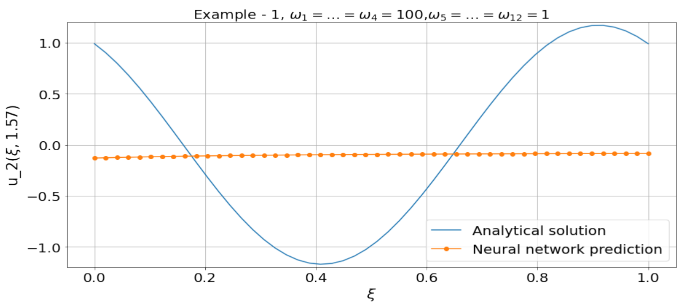

FIGURE 63. Graph of $u_2(\xi, 1.57)$

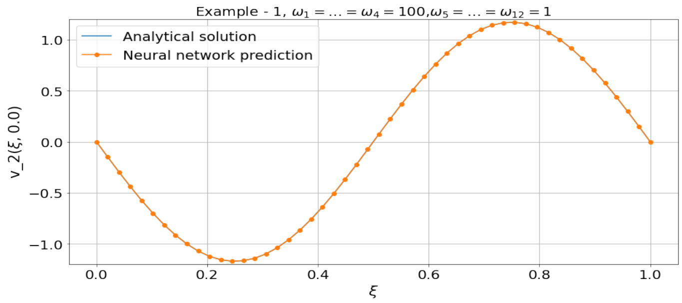

FIGURE 64. Graph of $v_2(\xi, 0)$

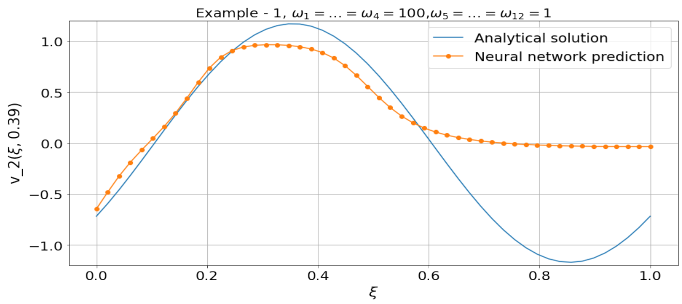

FIGURE 65. Graph of $v_2(\xi, 0.39)$

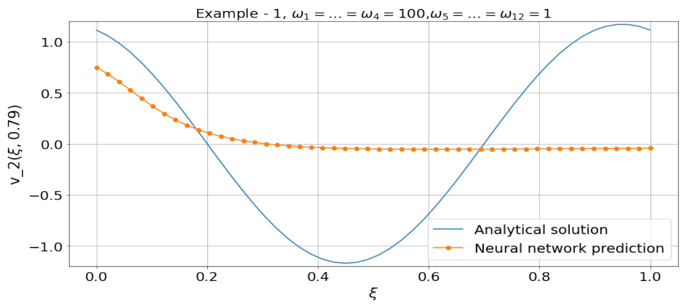

FIGURE 66. Graph of $v_2(\xi, 0.79)$

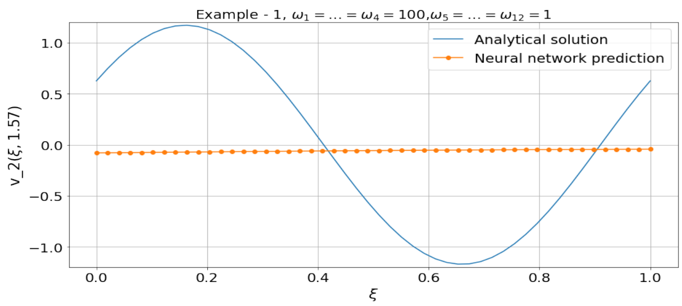

FIGURE 67. Graph of solution $v_2(\xi, 1.57)$

Referring to the graphs, we see that analytic and predicted solutions of linear Dirac equation in (1+1) dimension coincides at $\tau = 0.0$. However, at later time PINNs are not capable of providing good solutions. Also, boundary conditions are violated in many cases.

Now let's consider the case of

$$\omega_1 = \ldots = \omega_4 = 1, \omega_5 = \ldots = \omega_8 = 100, \omega_9 = \ldots = \omega_{12} = 1,$$

which puts more emphasis on mantaining the boundary conditions.

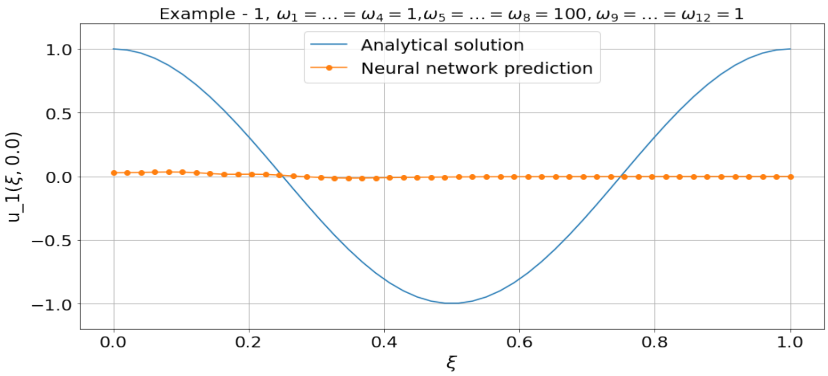

FIGURE 68. Graph of $u_1(\xi, 0)$

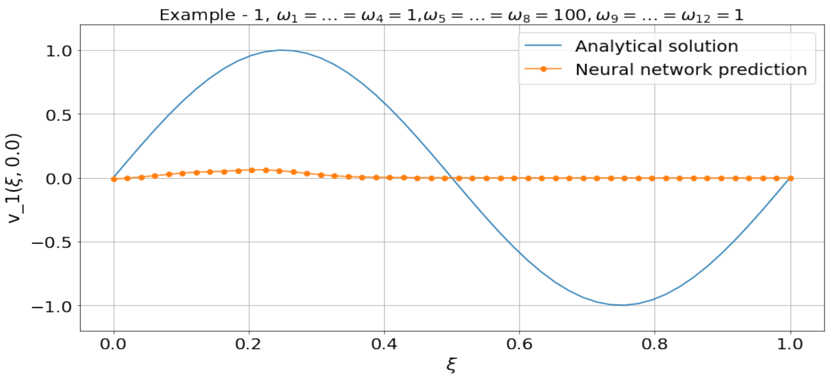

FIGURE 69. Graph of solution $v_1(\xi, 0)$

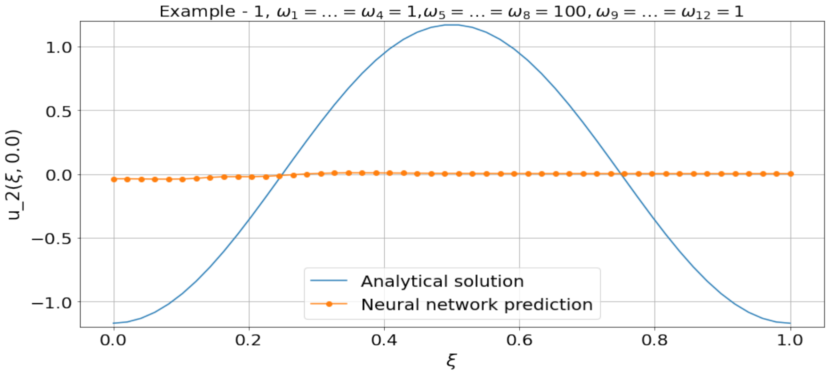

FIGURE 70. Graph of $v_1\,(\xi, 0)$

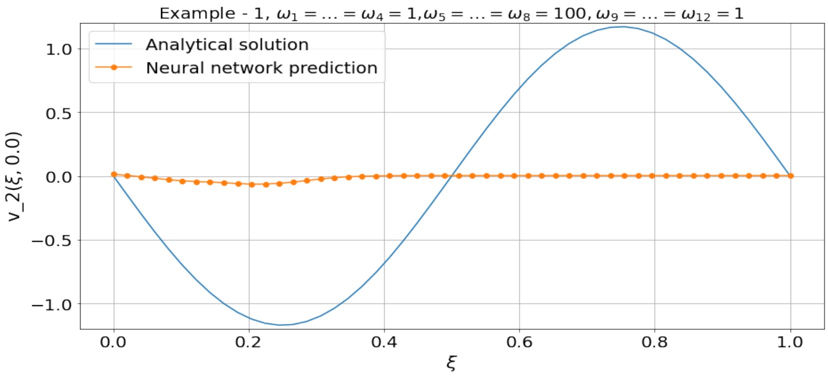

FIGURE 71. Graph of solution $v_2\,(\xi, 0)$

According to the obtained graphs, we see that making emphasis on boundary condition loss does not show good results at any given time. We did not check it for $\tau = 0.39$, $\tau = 0.79$, and $\tau = 1.57$, since it fails even at $\tau = 0.0$.

Now let's consider the case when $\omega_1 = \ldots = \omega_8 = 1, \omega_9 = \ldots = \omega_{12} = 100$

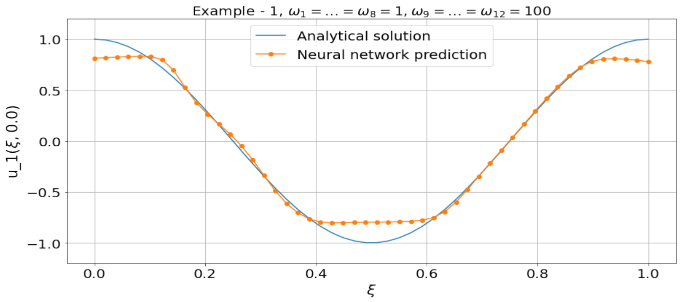

FIGURE 72. Graph of $u_1(\xi, 0)$

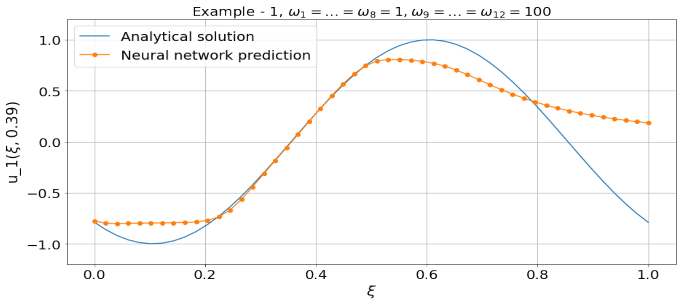

FIGURE 73. Graph of $u_1(\xi, 0.39)$

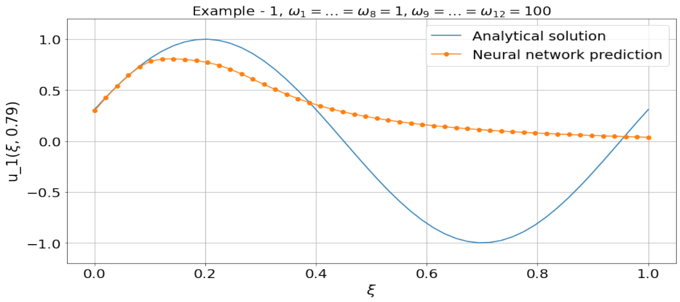

FIGURE 74. Graph of $u_1(\xi, 0.79)$

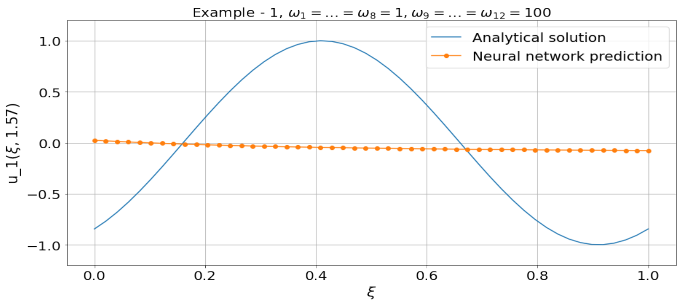

FIGURE 75. Graph of $u_1(\xi, 1.57)$

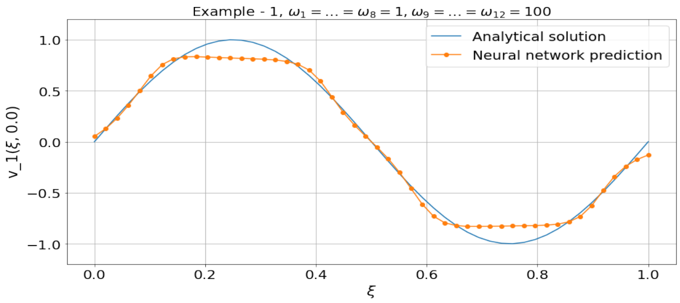

FIGURE 76. Graph of $v_1\,(\xi, 0)$

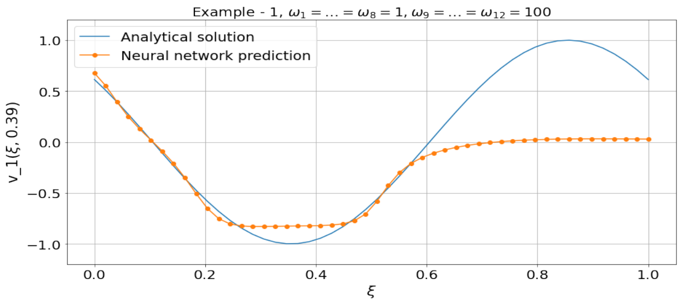

FIGURE 77. Graph of $v_1\,(\xi, 0.39)$

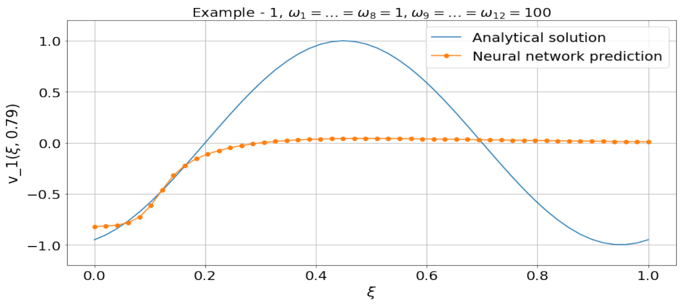

FIGURE 78. Graph of $v_1\,(\xi, 0.79)$

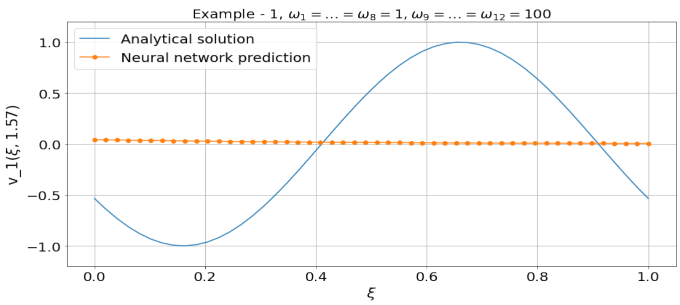

FIGURE 79. Graph of $v_1\,(\xi, 1.57)$

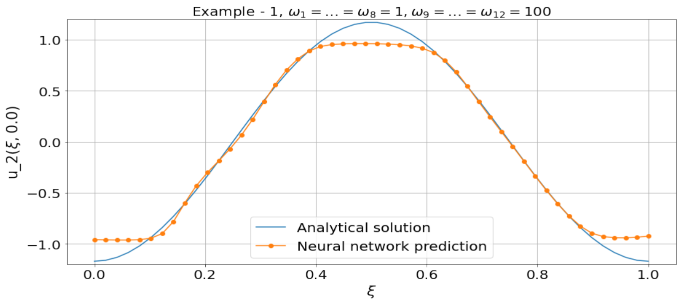

FIGURE 80. Graph of $u_2(\xi, 0)$

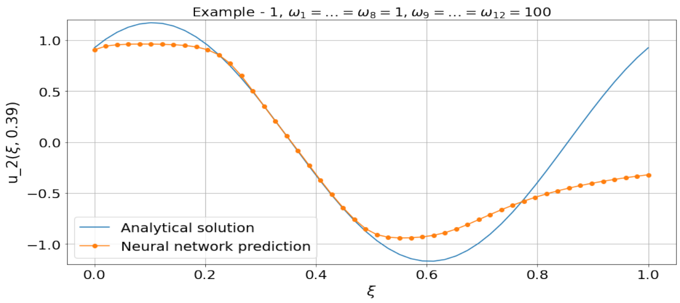

FIGURE 81. Graph of $u_2(\xi, 0.39)$

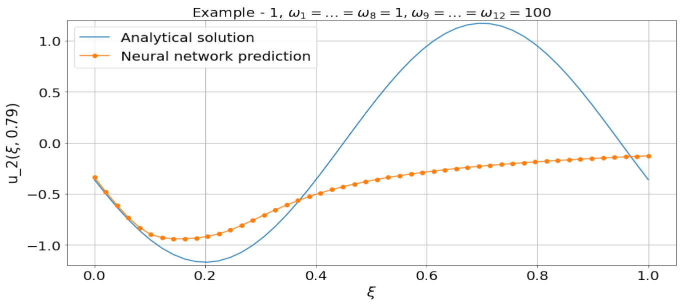

FIGURE 82. Graph of $u_2(\xi, 0.79)$

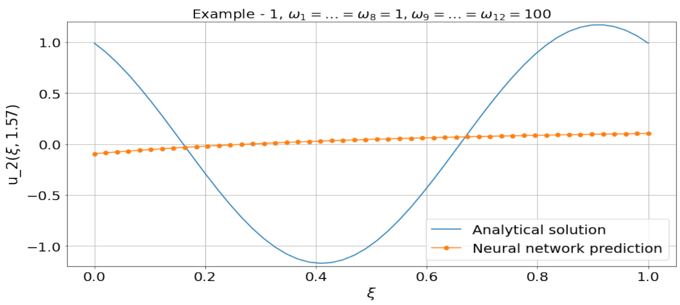

FIGURE 83. Graph of $u_2(\xi, 1.57)$

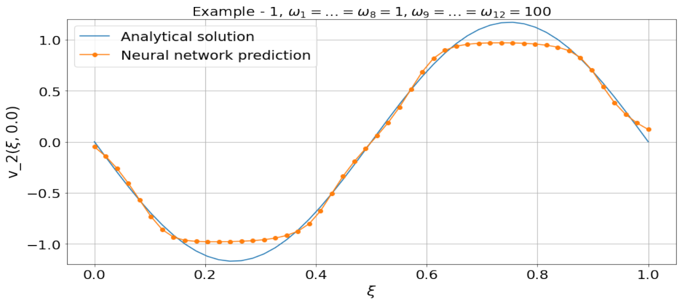

FIGURE 84. Graph of $v_2(\xi, 0)$

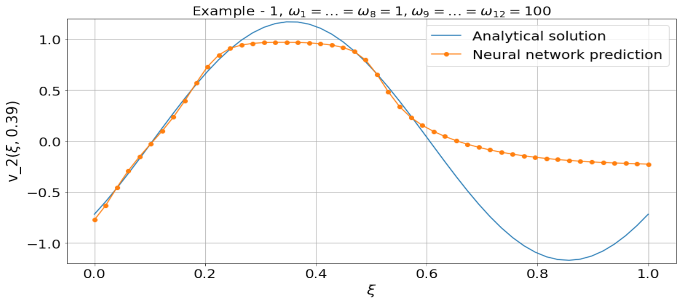

FIGURE 85. Graph of $v_2(\xi, 0.39)$

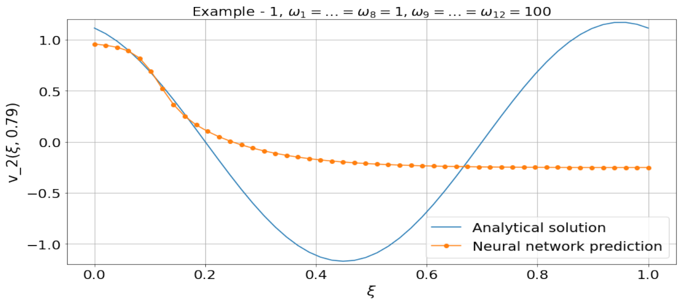

FIGURE 86. Graph of $v_2(\xi, 0.79)$

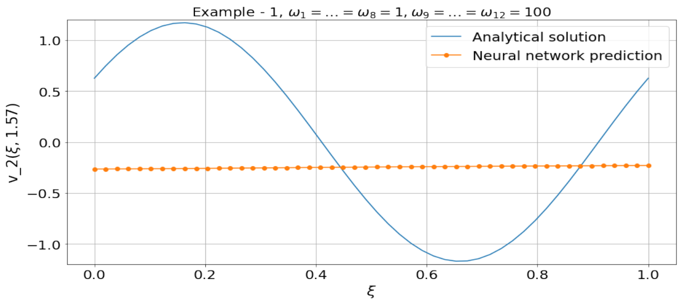

FIGURE 87. Graph of $v_2(\xi, 1.57)$

Referring to graphs we observe that putting emphasis on partial differential loss fails at $\tau = 0.39$. However, it shows better results than previous experiment on boundary condition loss.

4.3.2. *Experiment 2.* The purpose of this experiment is to test PINNs for the Example 2 and examine following cases:

- with emphasis on Initial Value Loss
- with emphasis on Boundary Condition Value Loss
- with emphasis on PDE Loss

and for each of them we test at times:

- $\tau = 0$,
- $\tau = \pi/8 \sim 0.39$,
- $\tau = \pi/4 \sim 0.79$,
- $\tau = \pi/2 \sim 1.57$.

Let's begin with the case $\omega_1 = \ldots = \omega_4 = 10000, \omega_5 = \ldots = \omega_{12} = 1$.

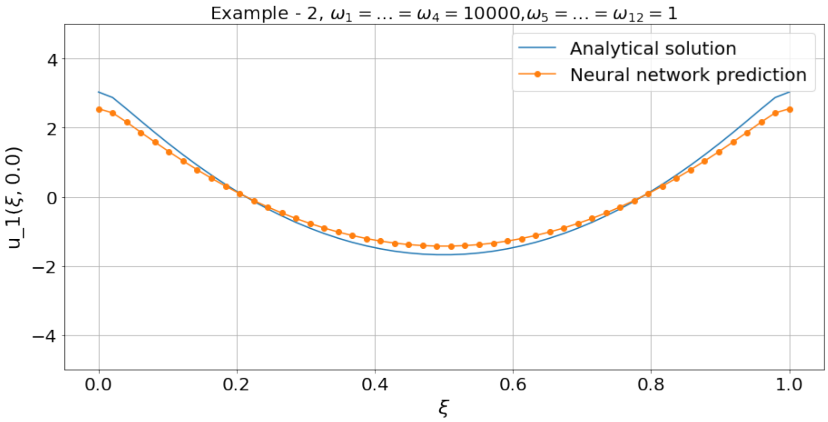

FIGURE 88. Graph of $u_1(\xi, 0)$

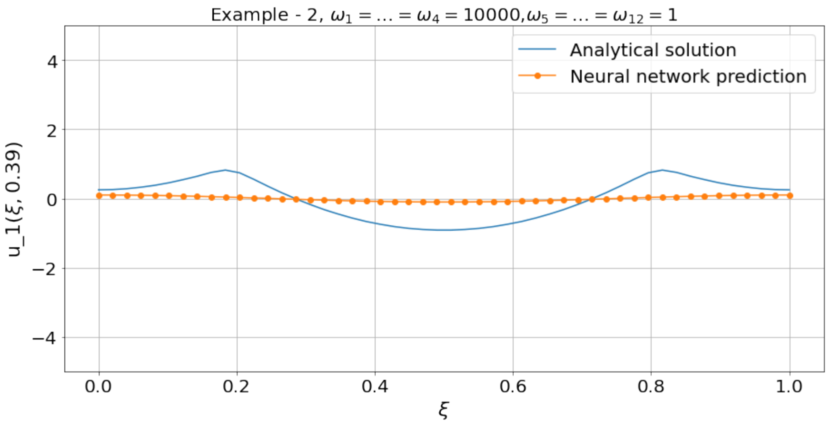

FIGURE 89. Graph of $u_1(\xi, 0.39)$

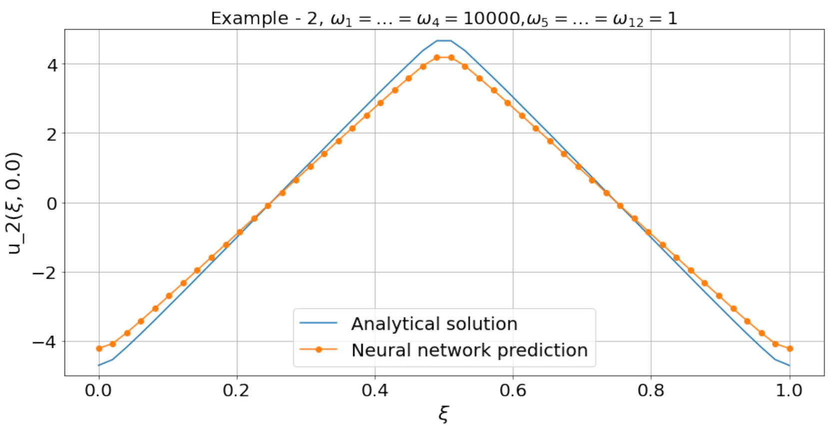

FIGURE 90. Graph of $u_2(\xi, 0)$

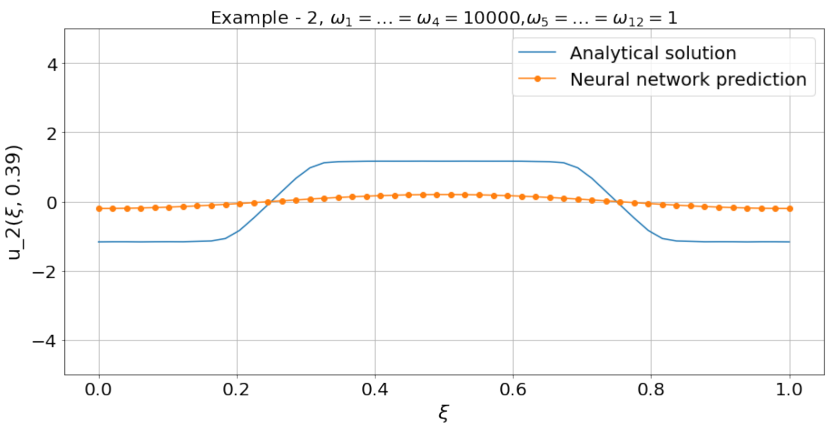

FIGURE 91. Graph of $u_2(\xi, 0.39)$

Observe that emphasis on initial value loss shows good accuracy only at $\tau = 0.0$ and at later times PINNs start to fail.

Now let's consider the case when $\omega_1 = \ldots = \omega_4 = 1, \omega_5 = \ldots = \omega_8 = 10000, \omega_9 = \ldots = \omega_{12} = 1:$

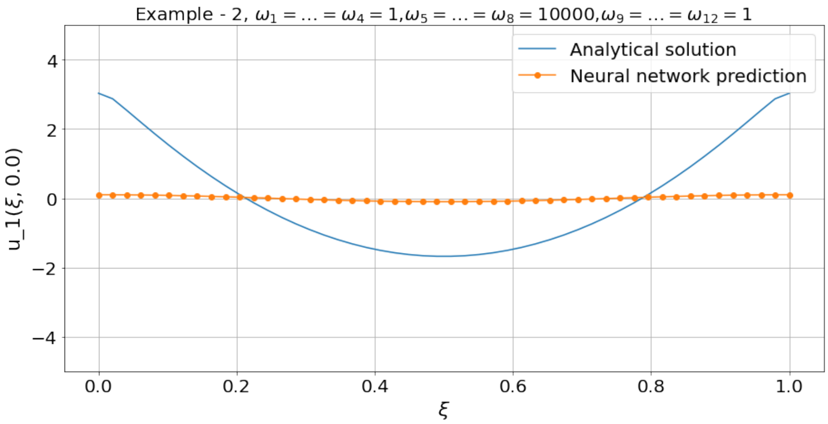

FIGURE 92. Graph of $u_1(\xi, 0)$

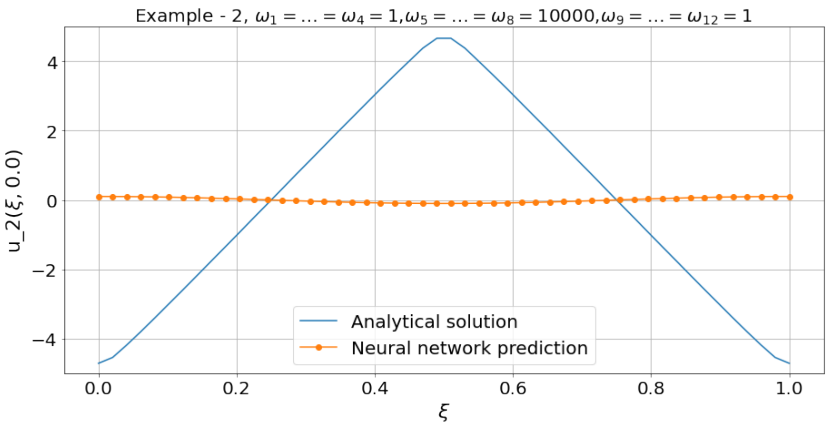

FIGURE 93. Graph of solution of $u_2(\xi, 0)$

Putting emphasis on boundary value loss converges to zero.

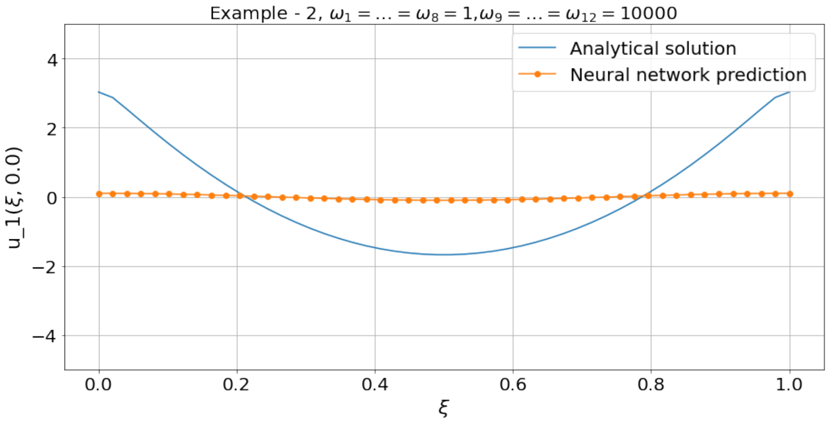

FIGURE 94. Graph of $u_1(\xi, 0)$

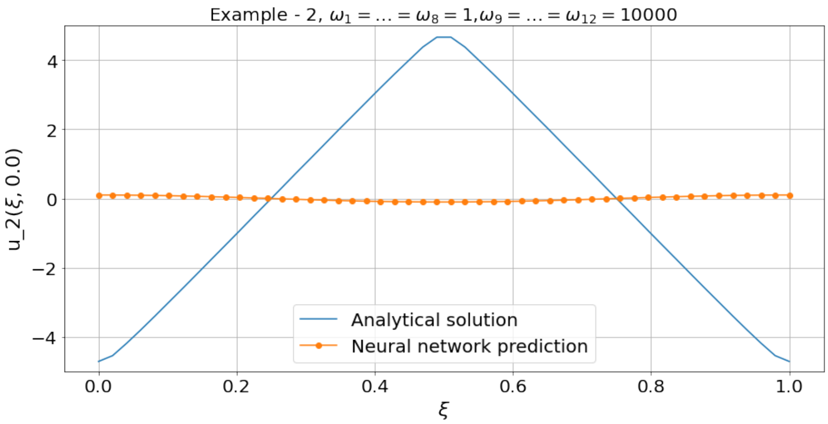

FIGURE 95. Graph of solution of $u_2(\xi, 0)$

Again we see that also putting emphasis on PDE loss does not provide satisfactory results.

4.3.3. *Experiment 3.* In this experiment we will test an example of initial boundary value problem for nonlinear Dirac equation in (1+1) dimension and its purpose is similar to previous experiments where we put emphasis on initial value, boundary value and PDE losses and check for times $\tau = 0, \quad 0.39, \quad 0.79, \quad 1.57.$

As usual, let's begin with the case $\omega_1 = \ldots = \omega_4 = 1000, \omega_5 = \ldots = \omega_{12} = 1:$

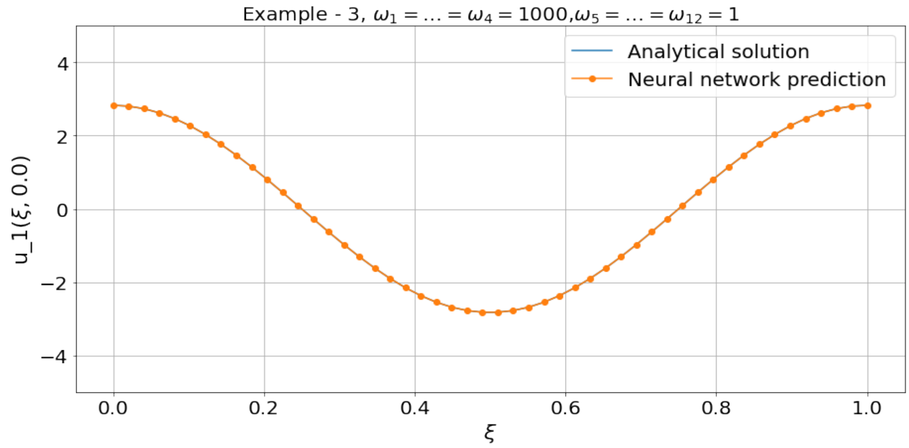

FIGURE 96. Graph of $u_1(\xi, 0)$

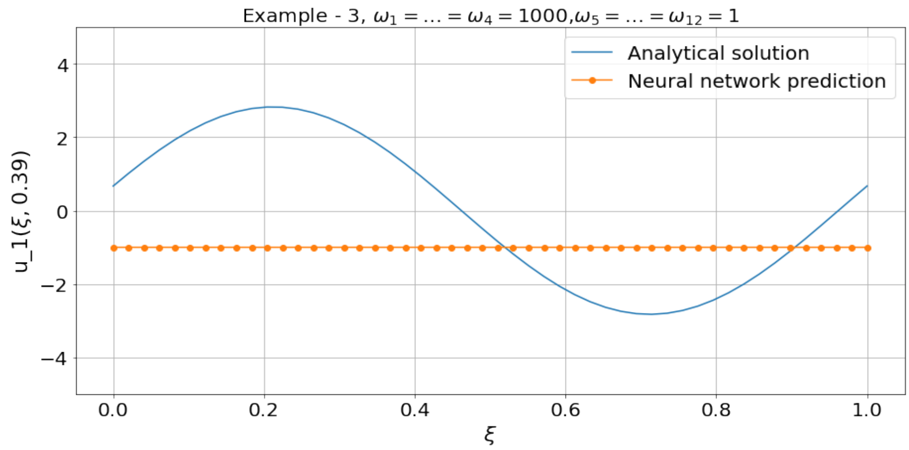

FIGURE 97. Graph of $u_1(\xi, 0.39)$

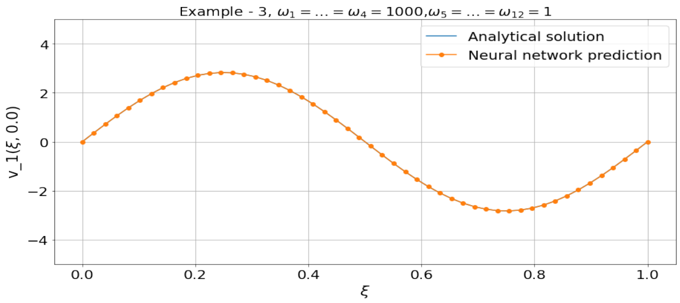

FIGURE 98. Graph of $v_1(\xi, 0)$

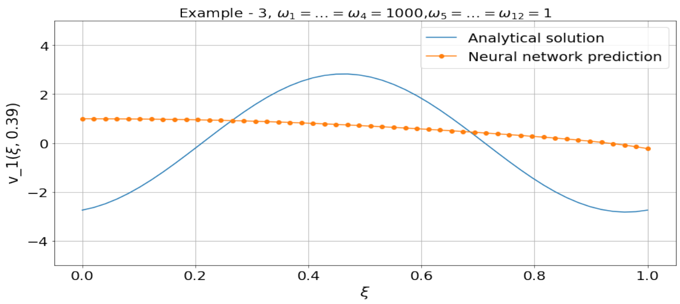

FIGURE 99. Graph of $v_1(\xi, 0.39)$

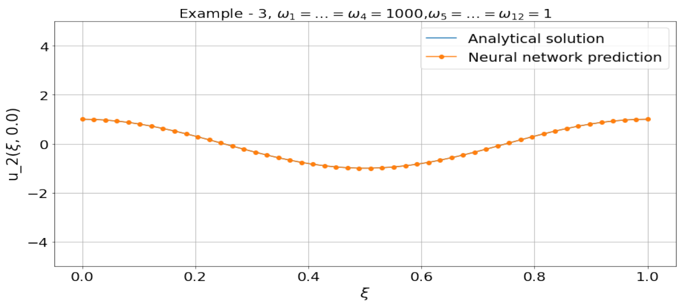

FIGURE 100. Graph of $u_2(\xi, 0)$

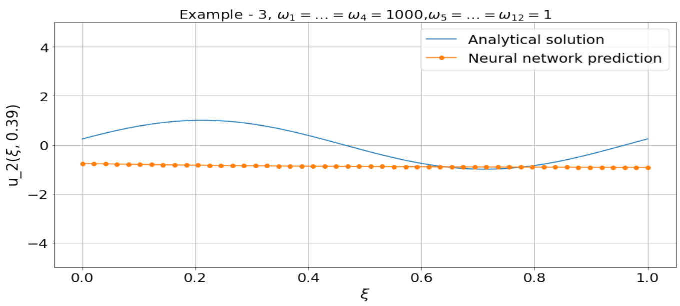

FIGURE 101. Graph of $u_2(\xi, 0.39)$

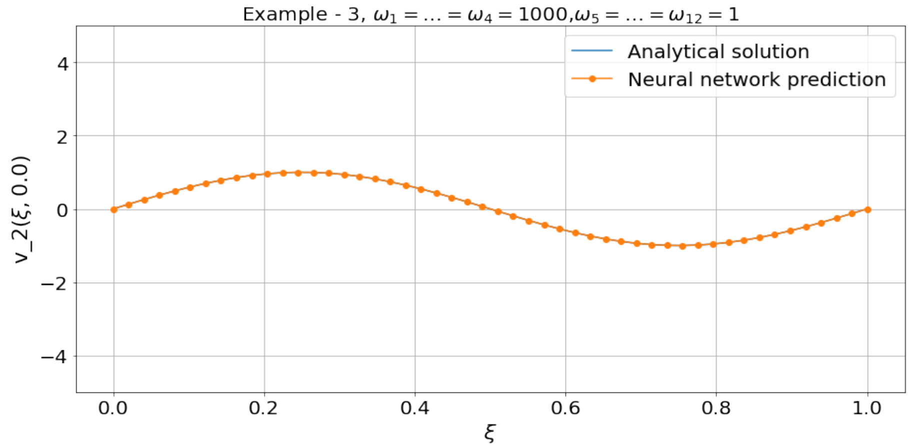

FIGURE 102. Graph of $v_2(\xi, 0)$

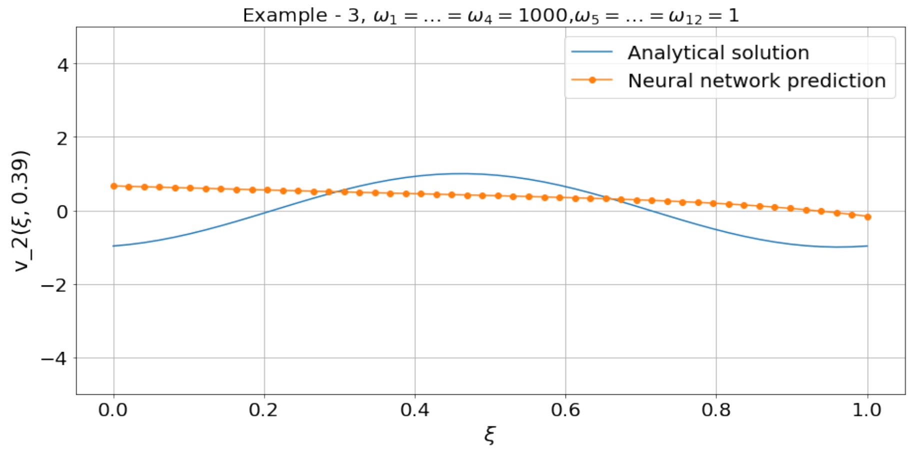

FIGURE 103. Graph of $v_2(\xi, 0.39)$

According to the obtained results, we observe that PINNs start to fail at $\tau = 0.39$. Hence we did not check for later times $\tau = 0.79$ and $\tau = 1.57$.

Now let's consider the case $\omega_1 = \ldots = \omega_4 = 1, \omega_5 = \ldots = \omega_8 = 1000, \omega_9 = \ldots = \omega_{12} = 1$:

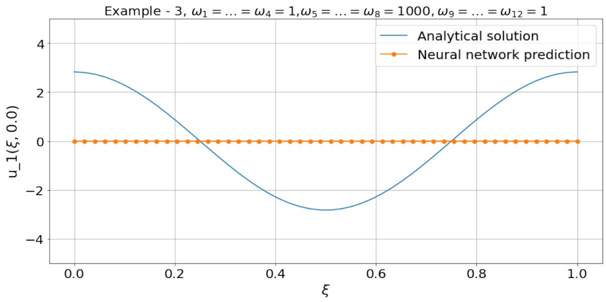

FIGURE 104. Graph of $u_1(\xi, 0)$

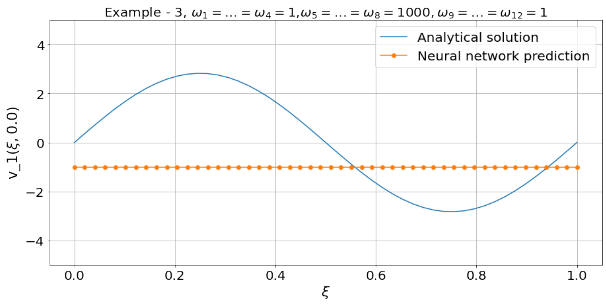

FIGURE 105. Graph of $v_1(\xi, 0)$

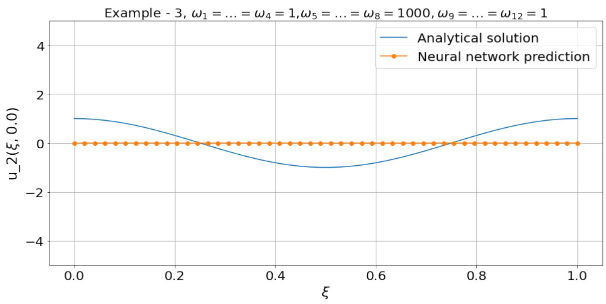

FIGURE 106. Graph of $u_2(\xi, 0)$

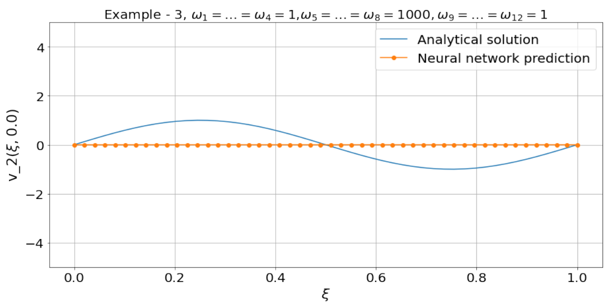

FIGURE 107. Graph of $v_2(\xi, 0)$

Observe that when we put emphasis on boundary value loss, PINNs totally fail.

Let's check for the case $\omega_1 = \ldots = \omega_8 = 1, \omega_9 = \ldots = \omega_{12} = 1000:$

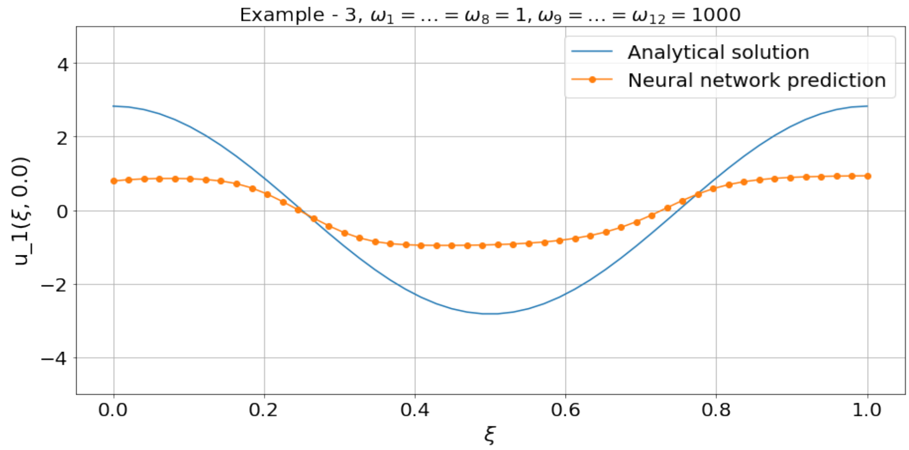

FIGURE 108. Graph of $u_1(\xi, 0)$

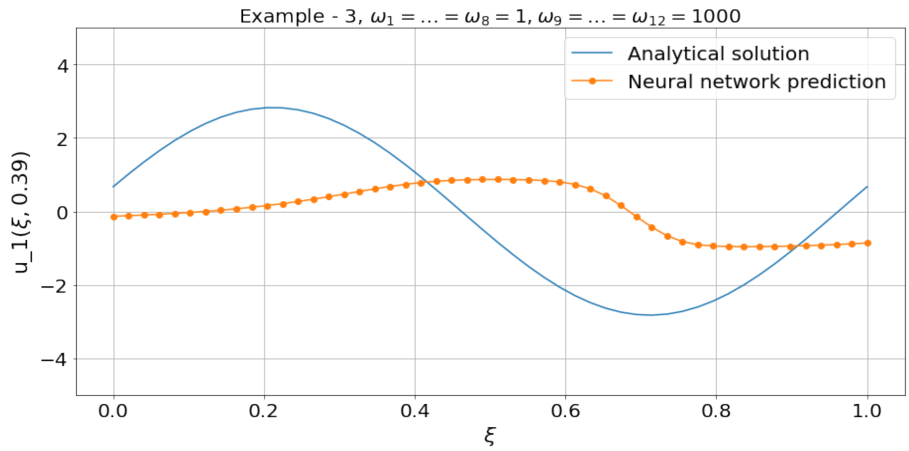

FIGURE 109. Graph of $u_1(\xi, 0.39)$

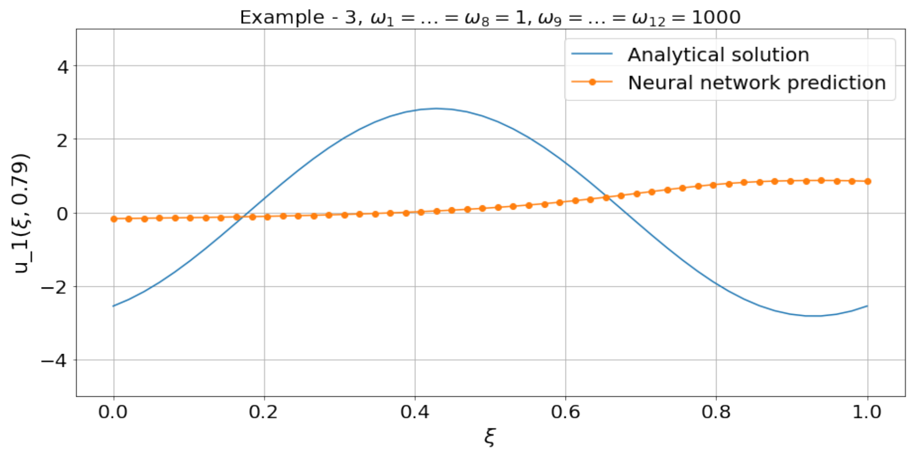

FIGURE 110. Graph of $u_1(\xi, 0.79)$

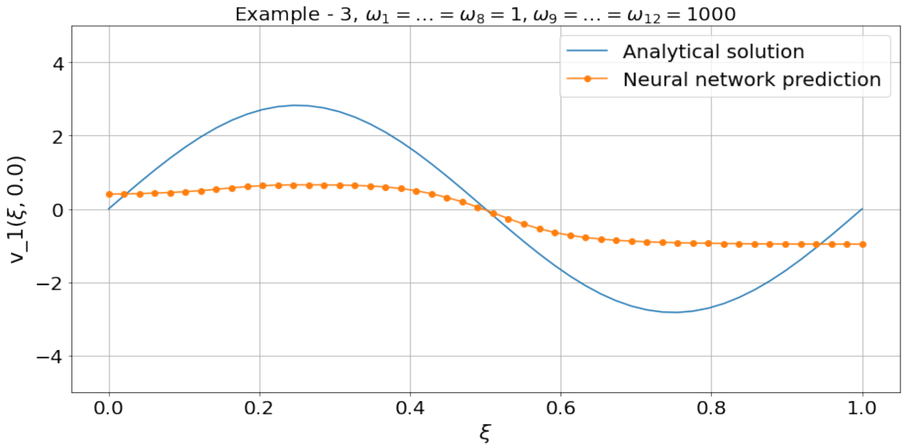

FIGURE 111. Graph of $v_1(\xi, 0)$

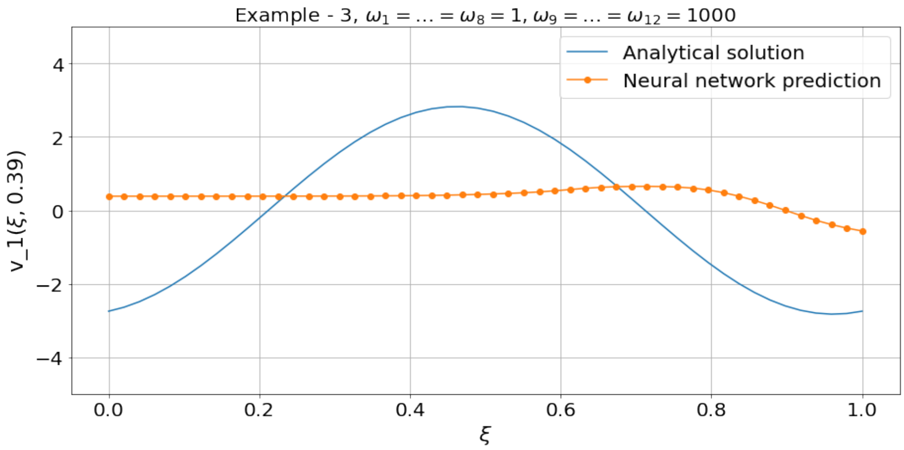

FIGURE 112. Graph of $v_1(\xi, 0.39)$

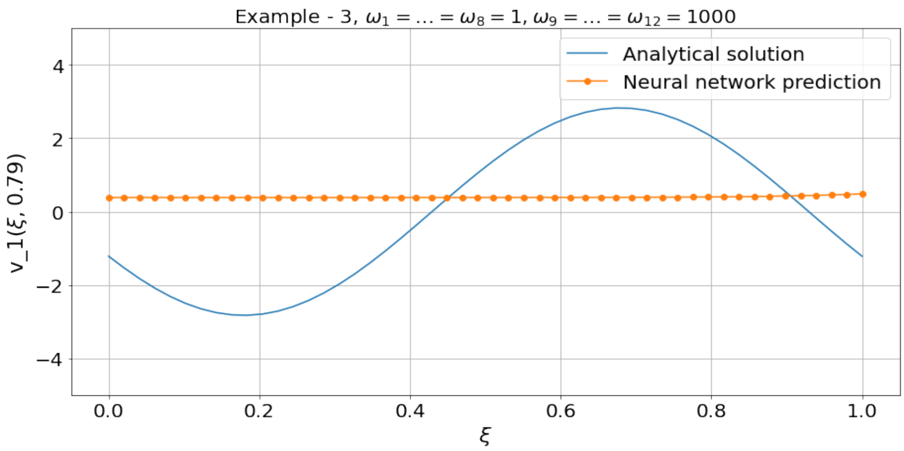

FIGURE 113. Graph of $v_1(\xi, 0.79)$

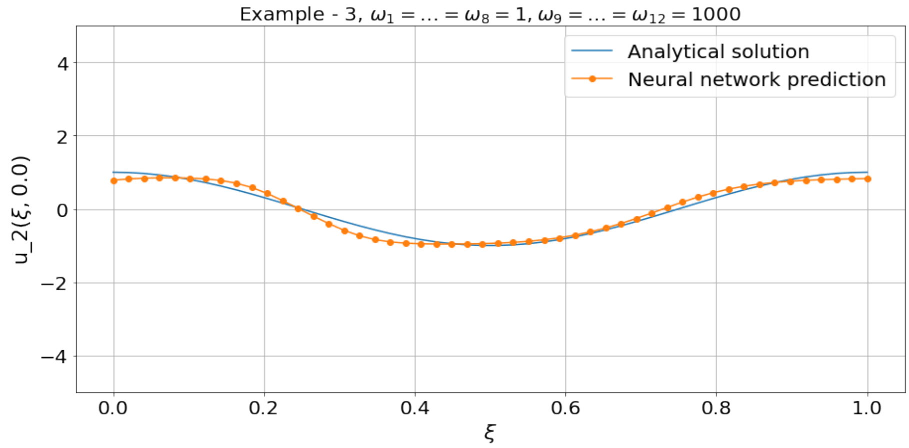

FIGURE 114. Graph of $u_2(\xi, 0)$

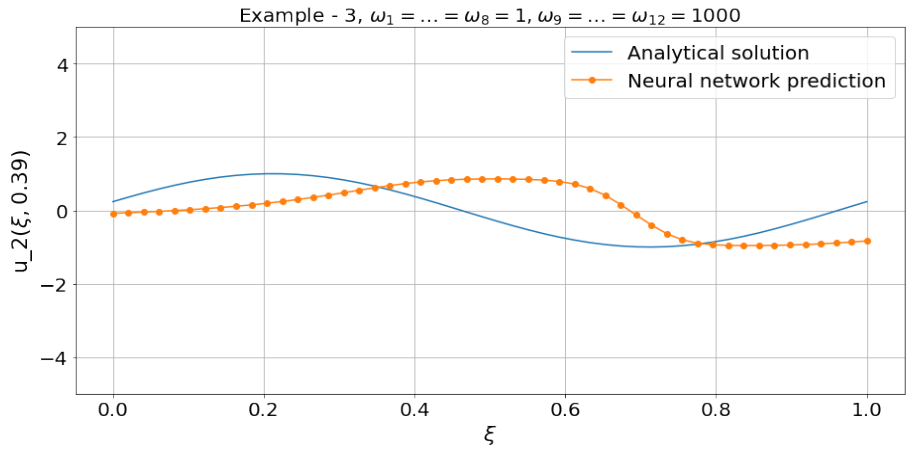

FIGURE 115. Graph of $u_2(\xi, 0.39)$

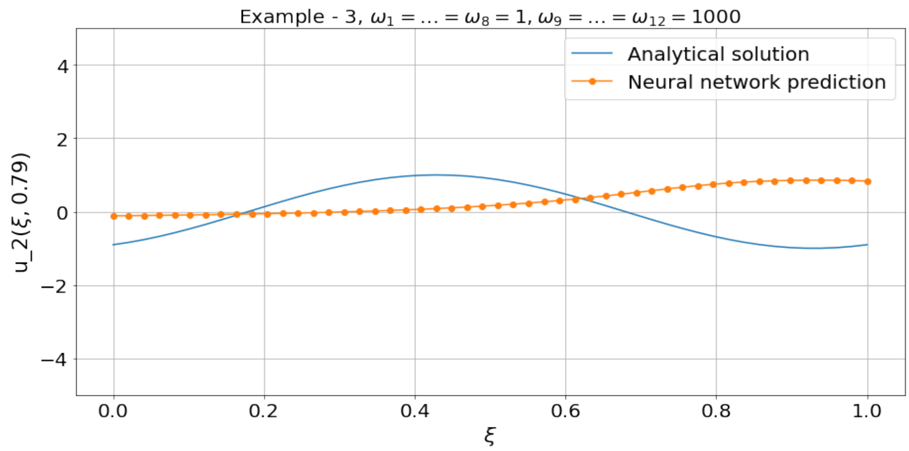

FIGURE 116. Graph of $u_2(\xi, 0.79)$

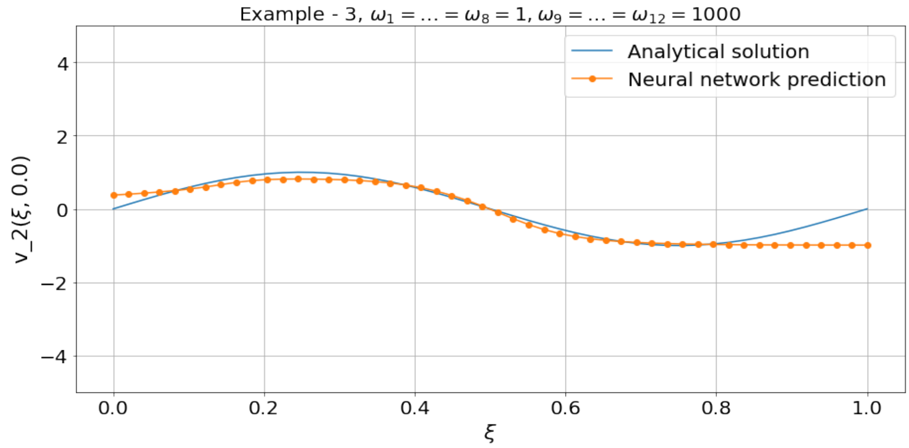

FIGURE 117. Graph of $v_2(\xi, 0)$

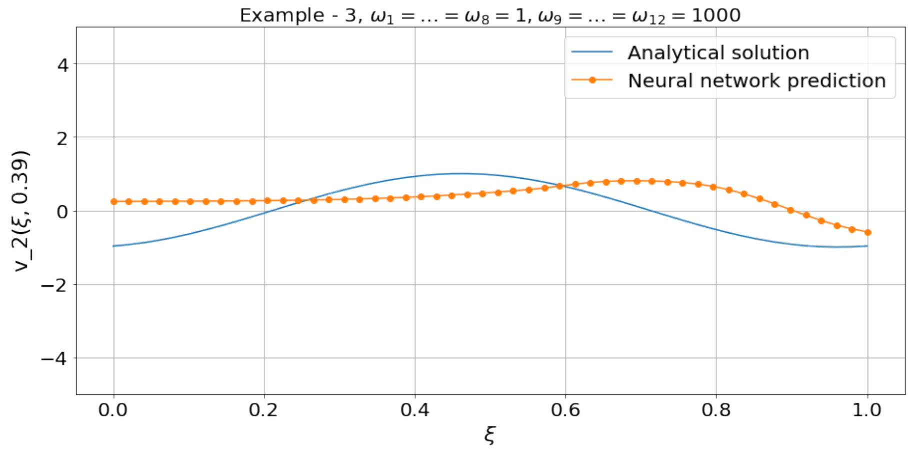

FIGURE 118. Graph of $v_2(\xi, 0.39)$

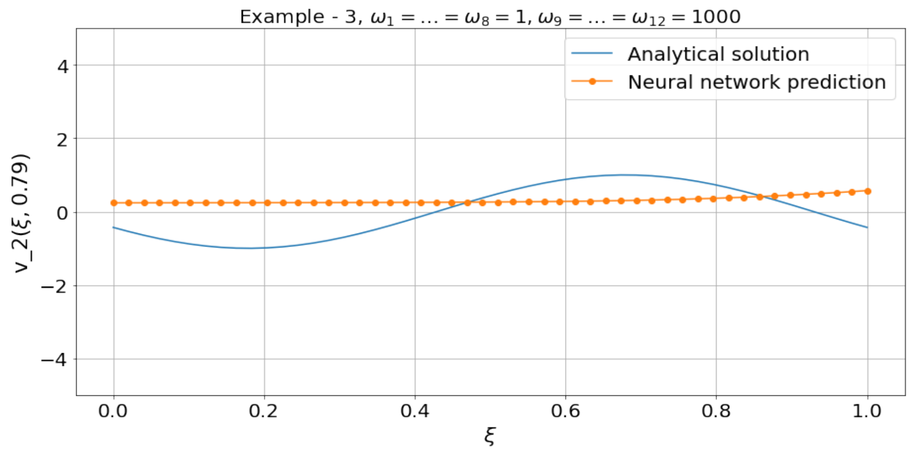

FIGURE 119. Graph of $v_2(\xi, 0.79)$

Note that for the last case of putting emphasis on PDE loss PINNs also fail at $\tau = 0.79$.

5. Conclusion

In our study we examine plane wave solutions of linear and nonlinear Dirac equation in (1+1) dimension. Solutions of initial value and initial boundary value problems have been obtained for Linear Dirac equation in (1+1) dimension and provided an example of initial boundary value problem for nonlinear Dirac equation in (1+1) dimension.

As for the machine learning part we followed idea of [14] where they have solved Burger's and Schrödinger equation applying PINNs and obtained good results using library Tensorflow 1. We reproduced their code to Tensorflow 2 and tested three examples applying Physics Informed Neural Networks. However, we note that PINNs are not always capable of solving any PDE since we have showed it for Dirac equation in (1+1) dimension. In all three experiments we observed that putting an emphasis on initial value loss and testing for $\tau = 0.0$ provides good solutions. However, at later times PINNs start to converge to zero. Moreover making emphasis on boundary condition and PDE loss totally lead to failure. Hence, further investigation is needed to make approximation of PINNs better and one of the attempts can be finding appropriate weights for each loss function.

References

[1] L. P. Aarts and P. Van Der Veer, *Neural network method for solving partial differential equations*, Neural Processing Letters, 14 (2001), pp. 261–271.

[2] V. G. Bagrov and D. Gitman, *Exact solutions of relativistic wave equations*, vol. 39, Springer Science & Business Media, 1990.

[3] W. E. Boyce, R. C. DiPrima, and D. B. Meade, *Elementary differential equations*, John Wiley & Sons, 2017.

[4] P. Collas and D. Klein, *The Dirac Equation in Curved Spacetime: A Guide for Calculations*, Springer, 2019.

[5] M. Dissanayake and N. Phan-Thien, *Neural-network-based approximations for solving partial differential equations*, communications in Numerical Methods in Engineering, 10 (1994), pp. 195–201.

[6] G. B. Folland, *Fourier analysis and its applications, Brooks*, 1992.

[7] W. Greiner et al., *Relativistic quantum mechanics*, vol. 2, Springer, 2000.

[8] K. Hornik, M. Stinchcombe, and H. White, *Multilayer feedforward networks are universal approximators*, Neural networks, 2 (1989), pp. 359–366.

[9] A. D. Jagtap, K. Kawaguchi, and G. E. Karniadakis, *Adaptive activation functions accelerate convergence in deep and physics-informed neural networks*, Journal of Computational Physics, 404 (2020), p. 109136.

[10] I. E. Lagaris, A. Likas, and D. I. Fotiadis, *Artificial neural networks for solving ordinary and partial differential equations*, IEEE transactions on neural networks, 9 (1998), pp. 987–1000.

[11] Z. Liu, Y. Yang, and Q. Cai, *Neural network as a function approximator and its application in solving differential equations*, Applied Mathematics and Mechanics, 40 (2019), pp. 237–248.

[12] S. Manzhos, *Machine learning for the solution of the schrödinger equation*, Machine Learning: Science and Technology, 1 (2020), p. 013002.

[13] I. Naumkin, *Cubic nonlinear dirac equation in a quarter plane*, Journal of Mathematical Analysis and Applications, 434 (2016), pp. 1633–1664.

[14] M. Raissi, P. Perdikaris, and G. E. Karniadakis, *Physics informed deep learning (part i): Data-driven solutions of nonlinear partial differential equations*, arXiv preprint arXiv:1711.10561, (2017).

[15] Y. Sabbah, U. Al Khawaja, and P. Vinayagam, *Lax pair and new exact solutions of the nonlinear dirac equation*, Communications in Nonlinear Science and Numerical Simulation, 61 (2018), pp. 167–179.

[16] Y. Shirvany, M. Hayati, and R. Moradian, *Multilayer perceptron neural networks with novel unsupervised training method for numerical solution of the partial differential equations*, Applied Soft Computing, 9 (2009), pp. 20–29.

[17] J. Sirignano and K. Spiliopoulos, *Dgm: A deep learning algorithm for solving partial differential equations*, Journal of computational physics, 375 (2018), pp. 1339–1364.

[18] S. Wang, X. Yu, and P. Perdikaris, *When and why pinns fail to train: A neural tangent kernel perspective*, arXiv preprint arXiv:2007.14527, (2020).

[19] Y. Zhang and Q. Zhao, *Initial boundary value problem for nonlinear dirac equation of gross-neveu type in 1+ 1 dimensions*, Journal of Mathematical Analysis and Applications, 477 (2019), pp. 708–733.